

**EFFECTS OF ASYMMETRIC TIP CLEARANCE ON
COMPRESSOR STABILITY**

by

Martin Bowyer Graf

B.S., Mechanical Engineering, University of Miami (Florida), 1990
S.M., Mechanical Engineering, Massachusetts Institute of Technology, 1993

Submitted to the Department of Aeronautics and Astronautics

in Partial Fulfillment of the Requirements for the

Degree of

MASTER OF SCIENCE IN AERONAUTICS AND ASTRONAUTICS

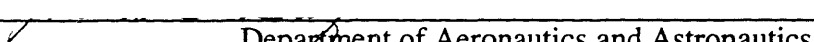
at the

Massachusetts Institute of Technology


June 1996

© Massachusetts Institute of Technology, 1996. All rights reserved.

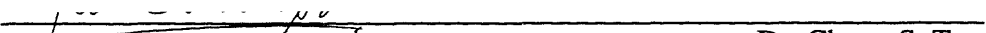
Signature of Author


Department of Aeronautics and Astronautics
May 24, 1996

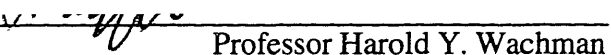
Certified by


Professor Edward M. Greitzer
H N Slater Professor of Aeronautics and Astronautics
Thesis Supervisor

Certified by


Dr. Choon S. Tan
Principal Research Engineer

Accepted by


Professor Harold Y. Wachman
Chairman, Departmental Graduate Committee

ARCHIVES
MASSACHUSETTS INSTITUTE
OF TECHNOLOGY

JUN 11 1996

LIBRARIES

EFFECTS OF ASYMMETRIC TIP CLEARANCE ON
COMPRESSOR STABILITY

by

Martin Bowyer Graf

Submitted to the Department of Aeronautics and Astronautics
on May 24, 1996 in Partial Fulfillment of the
Requirements for the Degree of Master of Science in
Aeronautics and Astronautics

ABSTRACT

Effects of asymmetric tip clearance on axial compressor stability have been investigated using a two-dimensional, incompressible, fluid dynamic stability model. Computations have been carried out to determine how the circumferential distribution of tip clearance, the compressor characteristic, and other system dynamic parameters affect the behavior of pre-stall disturbances and compressor stall margin.

The loss in stall margin associated with asymmetric tip clearance was found to be more severe than that based on the annulus averaged tip clearance. The loss in pressure rise capability was close to that seen with axisymmetric flow at the maximum clearance. Decreasing the length scale of the clearance non-uniformity mitigated the adverse effect on stall margin. The sensitivity to clearance asymmetry also depended on the compressor peak pressure rise and curvature of the characteristic. Compressor characteristics which were steep and had a sharp drop in pressure rise after the peak, promoted sensitivity to clearance asymmetry.

Thesis Supervisor: Edward M. Greitzer
Title: H. N. Slater Professor of Aeronautics and Astronautics

Thesis Co-Supervisor: Choon S. Tan
Title: Principal Research Engineer

Acknowledgments

Throughout the course of this project many individuals have provided me with motivation, guidance, and assistance. I would like to take this opportunity to thank all those who contributed, either directly or indirectly, to the completion of this work.

I would like to express my gratitude to Prof. E. M. Greitzer and Dr. C. S. Tan for their support, encouragement, and many thought provoking technical discussions. Thanks also to Prof. F. E. Marble for initially suggesting this problem, and for providing insightful questions and comments throughout, and to Prof. A. H. Epstein for his continued interest in this project.

Thanks to Mr. T. S. Wong for ensuring that the asymmetric clearance model gets put to the test.

Thanks to the past and present students of the GTL for their friendship and support, both of which have been greatly appreciated.

Thanks to my parents Robert and Leeda, and my sister Michelle, for their constant encouragement, love, and advice.

Finally, special thanks to Diane. For all you have done to help me finish, you have my respect, my gratitude, and my love. Thanks for everything.

The Air Force Office of Scientific Research provided funding for this work and for the author through the Air Force Research in Aero Propulsion Technology (AFRAPT) Fellowship program, Dr. J. McMichael, technical monitor.

Table of Contents

	Page
Abstract	2
Acknowledgments	3
List of Figures	6
Nomenclature	8
1. Introduction	
1.1 Background and Motivation	11
1.2 Review of Previous Work	14
1.3 Problem Statement and Research Objectives	16
1.4 Contributions of Thesis	17
1.5 Outline of Thesis	17
2. Compression System Model with Tip Clearance Asymmetry	
2.1 Introduction	21
2.2 Approach: Description of Model	21
2.3 Baseline Compressor Stability Calculations	26
2.4 Effect of Blade Row Unsteady Viscous Response	30
2.5 Effect of Compressor Characteristic Curvature	32
2.6 Effect of Compressor Peak Pressure Rise	33
2.7 Effect of Tip Clearance Asymmetry Distribution	33
2.8 Effect of Compressor\Compression System Coupling	35
3. Conclusions	
3.1 Summary and Conclusions	50
3.2 Implications of Present Work	51
3.2 Recommendations for Future Work	51

APPENDICES

(A) Equations in Compression System Stability Model

A.1 Steady Background Flow 55
A.2 Linearized Equations Governing Stability 56
A.3 Linearized Steady Flow with Clearance Asymmetry 60

(B) Formulation of Compressor Characteristics

B.1 Baseline Characteristics 63
B.2 Characteristics with Tip Clearance Asymmetry 64
B.3 Isentropic Characteristics 66

List of Figures

- 1.1a Single stage compressor characteristics with different clearances (McDougall [11])
- 1.1b Multi-stage compressor characteristics with different clearances (Wisler [9])
- 1.2 Schematic of compressor rotor with tip clearance flow
- 1.3a Loss in peak pressure rise capability with tip clearance size (Smith [6])
- 1.3b Loss in peak pressure rise capability with tip clearance size (Baghdadi [7])
- 1.4 Efficiency loss with tip clearance size (Wisler [13])
- 2.1 Schematic of compression system used for stability model
- 2.2 Baseline three-stage compressor pressure rise characteristic
- 2.3 Tip clearance distributions with uniform casing and 2% of chord cosine shaped asymmetry
- 2.4 Three-stage compressor characteristic family for 2% clearance asymmetry with peaks aligned
- 2.5 Three-stage compressor characteristic family for 2% clearance asymmetry with peaks along a 45 degree line
- 2.6 Flow coefficient distribution at compressor face at neutral stability for 2% cosine clearance asymmetry with characteristic peaks aligned
- 2.7 Pressure rise coefficient distribution at compressor face at neutral stability for 2% cosine clearance asymmetry with characteristic peaks aligned
- 2.8 Locus of operating points around annulus at neutral stability with characteristic peaks aligned
- 2.9 Pressure rise characteristic slope variation at neutral stability for 2% cosine clearance asymmetry with characteristic peaks aligned
- 2.10 Compression system eigenvalues at neutral stability
- 2.11 First mode wave envelope (flow coefficient perturbation) at neutral stability
- 2.12 Spectral content of first mode at neutral stability
- 2.13 Flow coefficient distribution at compressor face at neutral stability for 2% cosine clearance asymmetry with characteristic peaks along a 45 degree line

- 2.14 Locus of operating points around annulus at neutral stability with characteristic peaks along a 45 degree line
- 2.15 Locus of neutral stability point movement with cosine clearance variation
- 2.16 Effect of unsteady viscous loss response on neutral stability point movement with cosine clearance variation and characteristic peak shift
- 2.17 Effect of characteristic peak curvature on neutral stability point movement with cosine clearance variation and characteristic peak shift
- 2.18 Characteristics families of differing peak pressure rise (three, six, and nine stage machines) with 2% cosine clearance asymmetry and peaks aligned
- 2.19 Effect of compressor peak pressure rise on neutral stability point movement with cosine clearance variation and characteristic peak shift
- 2.20 Effect of tip clearance distribution on neutral stability point movement
- 2.21 Flow coefficient distribution at compressor face at neutral stability for 2% of chord $\cos(2\theta)$ clearance asymmetry with characteristic peaks aligned
- 2.22 Zeroth and first mode frequencies with and without clearance asymmetry
- 2.23 Ratio of Fourier components of first eigenmode at neutral stability with cosine clearance variation with characteristic peaks aligned
- 2.24 Loss in peak pressure rise capability with B - parameter
- 2.25 Change in flow coefficient at instability with B - parameter
- B.1 Schematic of actual and isentropic compressor pressure rise characteristics

Nomenclature

A	pressure rise characteristic coefficient, or area
A_n	Fourier coefficient
AR	blade aspect ratio
b_x	blade axial chord
B	Greitzer B - parameter, or a constant
B_n	Fourier coefficient
C	pressure rise characteristic coefficient
D	pressure rise characteristic coefficient
E	isentropic pressure rise characteristic coefficient
f	function
F	force
G	isentropic pressure rise characteristic coefficient
h	blade height
k	characteristic peak pressure rise shift parameter
k_t	throttle constant
L	aerodynamic loss
m	characteristic flow shift parameter
m, n	spatial harmonic number
N	number of compressor stages
P	pressure
r	radius
R	degree of reaction
t	time
T	fluidic inertia parameter for a blade row
U	rotor wheel speed
V	velocity
x	axial coordinate

Greek Symbols :

β	angle of characteristic peak line
γ	blade stagger angle
δ	boundary layer thickness
δ^*	displacement thickness
ε	tip clearance non-dimensionalized by chord
η	efficiency
θ	circumferential coordinate
λ	inertia of fluid in rotor
μ	inertia of fluid in compressor
ν	endwall tangential force defect
ϕ	flow coefficient
Φ	velocity potential function
ρ	density
τ	blade row viscous loss time constant
ψ	total-to-static pressure rise coefficient
ω	radian frequency

Subscripts :

1	at compression system inlet
2	at compressor face
3	at compressor exit
4	within plenum
5	at compression system exit
d	design point
h,t	hub or tip
i	isentropic
IGV	inlet guide vane
in	at inlet
m	hinge point
out	at outlet

p	peak point
r	rotor
s	stator
$total$	effective total length
ts	total-to-static
x	axial component

Superscripts :

–	averaged value
~	cascade value

Mathematical Operators :

i	complex number $\sqrt{-1}$
δ	perturbation
∂	partial derivative
∇	gradient
∇^2	Laplacian
$ $	absolute value
\Re	real part of complex quantity

Introduction

1.1 Background and Motivation

A major aspect of the overall performance of an axial compressor can be summarized by considering its mass flow versus pressure rise characteristic curve as shown in Figures (1.1a) and (1.1b) for a single stage and a multi-stage compressor respectively. The operating range of these turbomachines is limited at low mass flow rates (high pressure rise) by the onset of fluid dynamic instability. As the flow rate is reduced, the pressure rise across the compressor typically increases monotonically until an instability is encountered. When this occurs, the steady, essentially axisymmetric flow through the system rapidly transitions to an unsteady, generally non-axisymmetric flow, with large amplitude oscillations. There is also a concomitant decrease in time mean pressure rise and mass flow as compared to the values prior to instability.

Although the detailed structure of the aerodynamic instability can take several forms depending upon compression system parameters, the instabilities can be put two broad classes: (a) surge, or (b) rotating stall [1, 2]. The first of these is a global system instability which is characterized by large scale roughly one-dimensional oscillations in compressor flow and pressure rise, including periods of flow reversal through the machine. The second type, rotating stall, is local to the compressor and is a two- or three-dimensional disturbance associated with separation of flow from a region of airfoils around the compressor annulus. This patch of separated or reversed flow propagates around the annulus as a result of incidence variations on airfoils adjacent to it [3]. The axial extent of

the non-axisymmetric disturbances associated with rotating stall is typically confined to the compressor, but the resultant behavior of the overall system is to operate at reduced time mean pressure rise and mass flow. Experiments have shown that the frequency of surge oscillations is on the order of a few hertz while that of fully developed rotating stall is typically one-quarter to half the rotor rotational frequency [5].

In 1976, Greitzer [4, 5] showed analytically and experimentally that the form the instability takes in its mature state (surge or rotating stall) is related to a non-dimensional system parameter. This parameter, denoted by B , is defined as the ratio of fluidic compliance to fluidic inertia within a particular pumping system. In both a theoretical [4], and an experimental [5] study, Greitzer demonstrated that compression systems with low B values exhibit rotating stall, while those with large B undergo surge oscillations.

Both forms of instability severely degrade compression system performance and durability, and to avoid them a compression system must be operated at a safe margin from the point where the instabilities occur (“a stall/surge margin”). Since the instability point is often near the operating points with the greatest pressure rise and efficiency, this constraint is generally observed at the cost of overall compression system performance.

Considerable work has been done to determine which geometric and aerodynamic factors most influence compressor stability and off-design performance. Of the various features identified, compressor rotor tip clearance, which is the gap between the rotating blade tip and the stationary outer casing, has been found to be one of the most important in determining the performance of a given machine.

Figure (1.2) shows a schematic of the tip clearance flow. Due to the pressure difference across the rotor blade tip, leakage flow goes from the pressure side of the airfoil over the blade to the suction side. The clearance flow then rolls up to form a vortex somewhat analogous to the wing tip vortices on aircraft. The tip leakage vortex is characterized by high stagnation pressure loss and low axial momentum. Hence it cannot

withstand a strong adverse pressure gradient without large increases in cross-sectional area, i.e. aerodynamic “blockage”.

One of the earliest compilations of experimental data which demonstrates the importance of rotor tip clearance on compressor pressure rise capability is that of Smith [6]. Figure (1.3a) from [6] shows, for a number of compressors with clearances between 1.5 and 8% of chord, a 1% increase in clearance produces approximately a 5% decrease in peak pressure rise¹. Figure (1.3b) shows more recent data from Baghdadi [7] which also provides a trend similar to the data of Smith [6]. The trends illustrated in these figures have been also been corroborated by data from other sources including Koch [8], Wisler [9] and [10-12].

In addition to the effect on pressure rise capability, there is also an impact on machine efficiency as shown in Figure (1.4) from Wisler [13]. Efficiency penalties range from 1 to 2 points for each 1% increase in the stage average clearance/blade height, depending upon the design. Over the years, data such as these have provided strong motivation to understand the nature of the tip clearance flow field as well as to develop techniques to modify it.

In spite of the importance of the tip clearance flow, however, complete explanations of the mechanisms by which the endwall flow degrades blade row performance still do not exist, and the present status is that empirical correlations are employed in the design process. In addition, although there is a strong connection between compressor tip clearance, system stability, and off-design performance, the relevant fluid dynamic mechanisms are still poorly understood.

¹ For clearance/chord less than 1.5%, the sensitivity to clearance change is also observed, however data appears less conclusive regarding the magnitude of the change in pressure rise capability.

1.2 Review of Previous Work

This thesis examines the stability of a compression system with circumferentially non-uniform tip clearance. The investigation is based on compression system stability modeling coupled with the data regarding the effects of tip clearance on compressor performance. The review of previous work is limited to that which has had a strong influence on the present study.

Since the pioneering work of Emmons et al [3] the topic of compressor surge and stall has been extensively studied by numerous researchers. An indication of some of the work done in this area can be gathered by examining the reviews of Greitzer [1, 2].

Since these reviews a number of studies have been published regarding the modeling of surge and stall in compression systems. Of these the works of Moore [14] and Moore and Greitzer [15, 16] formed the basis for many subsequent investigations. These investigations furthered the idea that surge and rotating stall were actually large amplitude, limit cycle oscillations of initially small amplitude, essentially linear, instabilities. As the initial velocity or pressure disturbances grow, the flow field of the compression system was predicted to evolve from axisymmetric through-flow to fully developed rotating stall. The form of disturbance utilized in these models were annulus circumference scale, traveling waves which may contain several spatial harmonics. The Moore-Greitzer model as initially developed assumed the existence of such waves in a compression system with uniform inlet conditions.

To examine the effects of circumferentially non-uniform (distorted) inlet flow on compression system stability, Mazzawy [17] developed a model which was based on parallel compressor theory. This study showed that adequate predictions of performance degradation with inlet distortion could be obtained by modeling the different circumferential locations as a number of separate (parallel) compressors coupled together. Later, linear and nonlinear models based on the work of Moore and Greitzer, were also developed by Hynes and Greitzer [18], Longley [19], Strang [20] and Chue et al [21] to examine the effects of

stationary and rotating inlet distortions. These studies identified parametric dependencies linking the stability of a compression system operating with inlet distortion to aerodynamic and geometric design variables.

A review of the Moore-Greitzer type stability models for compression systems with uniform and distorted inlet flow has recently been given by Longley [22]. The review also addressed additional phenomena which are frequently incorporated to improve stability predictions; including unsteady blade row loss time lags, blade row deviation effects, and variations in inlet and exit swirl.

A fundamental assumption of the Moore-Greitzer type models is the presence of circumferential traveling waves prior to compression system instability. The existence of such waves has been confirmed by a number of experimental studies in single and multi-stage compressors. Experiments on low speed single stage compressors with undistorted inlet flow which show traveling disturbances include those of McDougall et al [11], Garnier et al [23], Paduano et al [24], and Gysling and Greitzer [25]. Similarly, low speed multi-stage measurements by Garnier et al [23] and Haynes et al [26] also show the presence of traveling waves, as do the studies of Longley [19] and Longley et al [27] for compressors with stationary and rotating inlet distortions. Pre-stall traveling disturbances have also been observed in some high speed compressors as shown by Garnier et al [23] and Tryfonidis et al [28].

Although these experiments lend confidence to the traveling wave (sometimes referred to as “modal”) type stability models, other studies of rotating stall inception have demonstrated that a different mechanism may lead to instability. The work of Day [29] has shown that for some compressors, rotating stall appears to emerge from a localized, finite amplitude, three-dimensional disturbance which contains significant span-wise non-uniformity. The formation of these non-modal traveling disturbances is not captured by the “two-dimensional” stall inception process described by the Moore-Greitzer model.

At present, the compression system parameters which determine the nature of the stall inception process (either two- or three-dimensional) have not been clearly identified. Hence, for a particular compression system the form of the disturbance leading to instability must be determined experimentally. However, for many low speed compressors, the data indicate that models based on work of Moore-Greitzer can capture the primary phenomena leading to instability.

There is much less work on the effects of tip clearance non-uniformity on compressor performance. Horlock and Greitzer [29] conducted a linearized analysis to compute velocity disturbances induced by clearance asymmetry, and their results indicated that sizable flow non-uniformities can be generated by clearance non-uniformity. The generation of structural forces as result of non-uniform clearance has been addressed by Colding-Jorgensen [31] using an extension of the Horlock-Greitzer model [29], and by Ehrich [32] using a parallel compressor model. These studies did not pursue a model for the impact on compressor stability, and thus a goal of the present work was to develop a methodology to predict the effects of tip clearance non-uniformity on compression system performance and stability.

The ability to predict and measure instability precursors (i.e. traveling disturbances) has provided an opportunity to apply methods based on closed loop control to modify the stability and operating characteristics of compression systems. This concept was first proposed by Epstein et al [33], and a number of studies since have demonstrated the feasibility of such control. A recent summary of some of the control schemes employed to stabilize compression systems is provided by Paduano et al [34].

1.3 Problem Statement and Research Objectives

This thesis examines the influence of non-uniform tip clearance on compression system stability and off-design performance.

The objectives for the investigation are:

- Formulate a mathematical compression system stability model that includes tip clearance asymmetry.
- Utilize the model to elucidate the effects of clearance asymmetry on the compressor flow field and stability.

Specific fluid dynamic questions to be addressed are:

- Is the effect of tip clearance asymmetry to cause the stability of the system to differ from that based on average clearance? If so, why?
- How is the compressor stability limit affected by the tip clearance distribution and other system parameters?

1.4 Contributions of Thesis

A new model has been created to predict the effects of asymmetric tip clearance on the compressor flow field and stability. Through numerical simulations it was found the loss in stall margin associated with asymmetric tip clearance was more severe than that based on the annulus averaged tip clearance. A sensitivity study has also been conducted to determine how the clearance distribution and other system parameters effect stability limits. The model has been used to design an experiment on the a multi-stage compressor which is being carried out at the GE Aerodynamics Research Laboratory.

1.5 Outline of Thesis

The thesis is organized in the following manner:

Chapter 2 provides the description, development, and application of a model for determining the effect of tip clearance asymmetry on compressor stability. A parametric study of compressor and system parameters is also included. Chapter 3 presents conclusions, implications of this study, and recommendations for future work. Appendix A gives the equations employed in the stability model, and Appendix B provides the mathematical formulation utilized to incorporate the effects of tip clearance asymmetry.

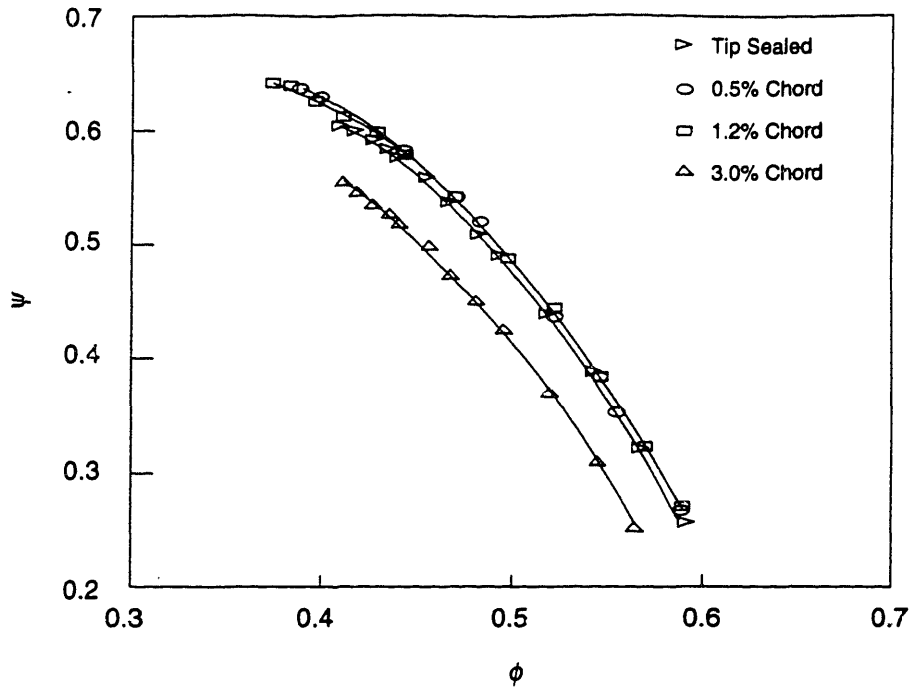


Figure (1.1a): Single stage compressor characteristics (McDougall [11])

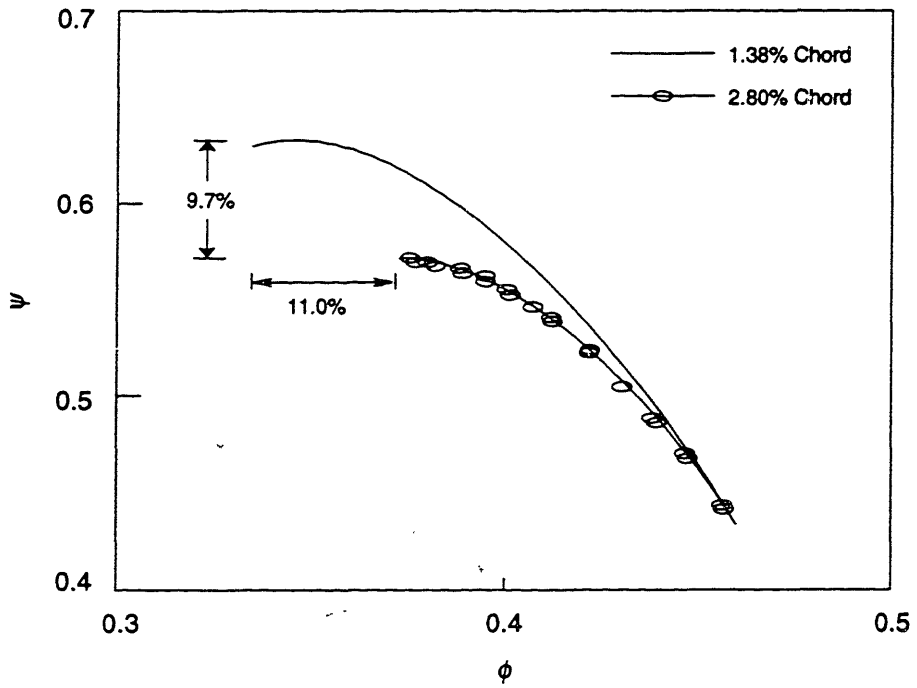


Figure (1.1b): Multi-stage compressor characteristics (Wisler [9])

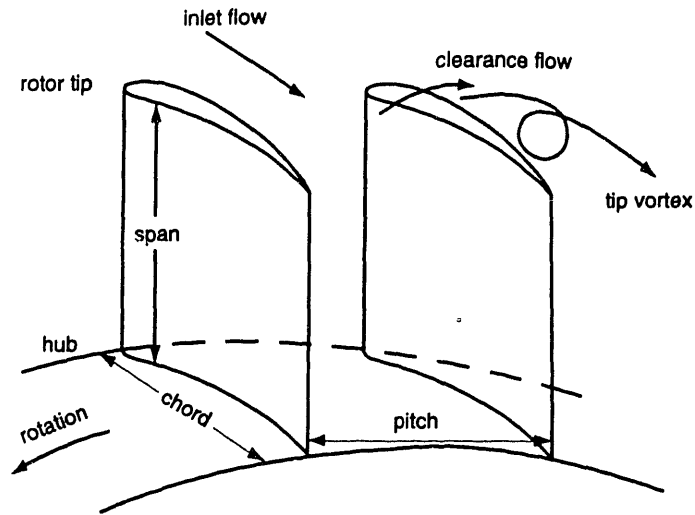


Figure (1.2): Schematic of compressor rotor with tip clearance flow (casing not shown)

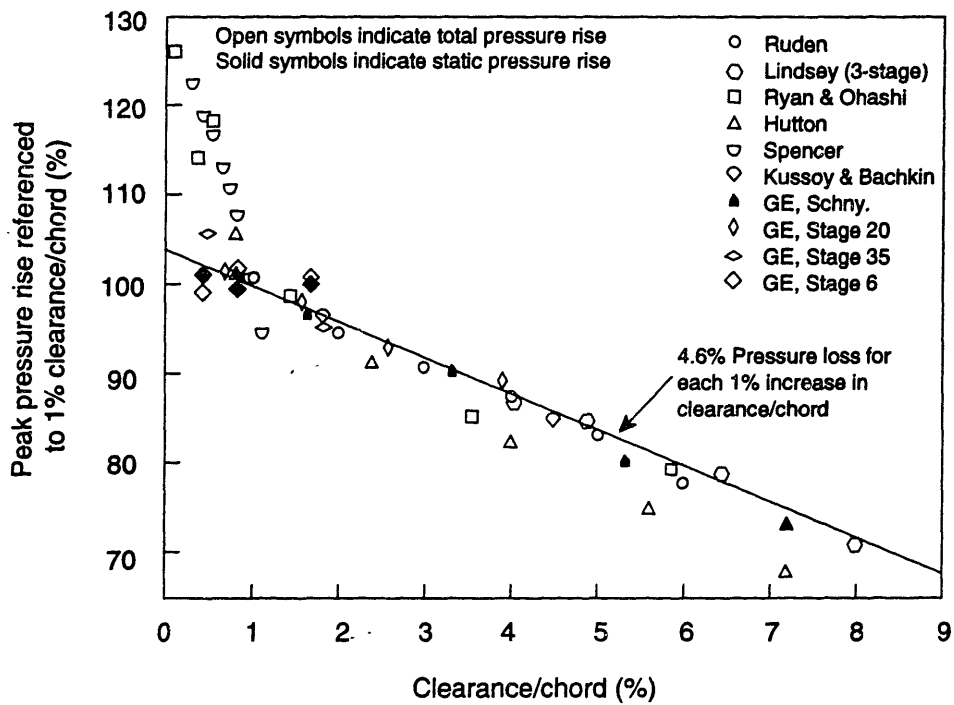


Figure (1.3a): Loss in peak pressure rise capability with tip clearance size (Smith [6])

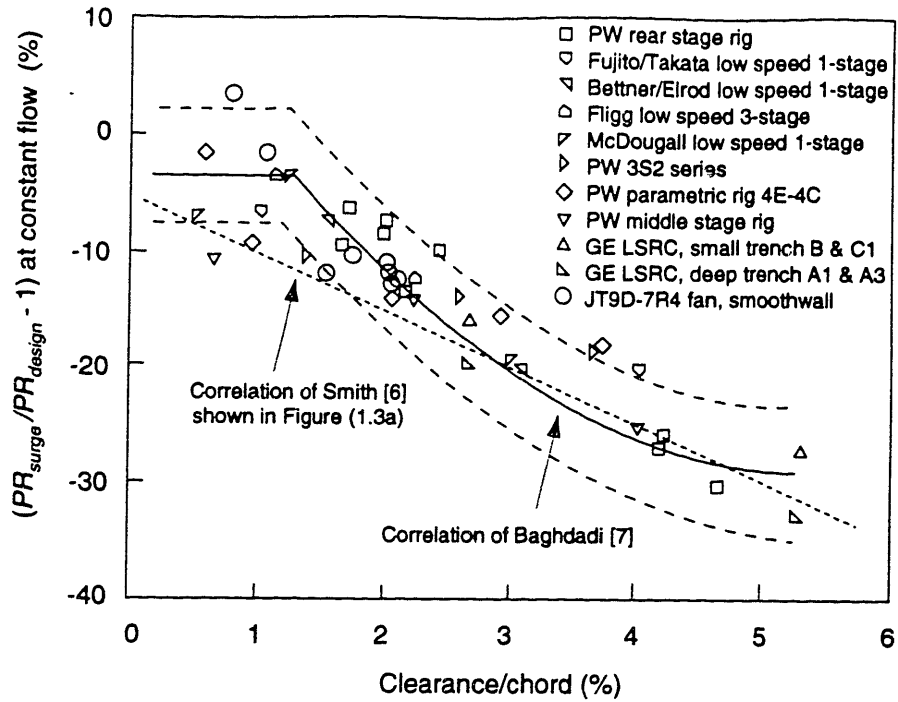


Figure (1.3b): Loss in peak pressure rise capability with tip clearance size (Baghdadi [7])

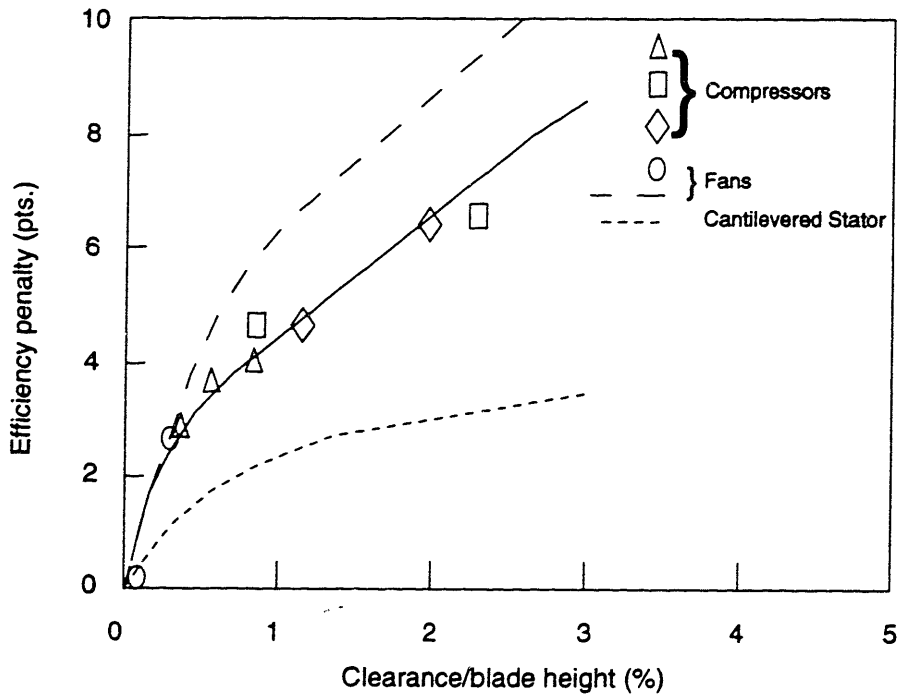


Figure (1.4): Efficiency loss with tip clearance size (Wisler [13])

Compression System Model with Tip Clearance Asymmetry

2.1 Introduction

Although there has been a considerable amount of work on the effects of axisymmetric tip clearance size on compressor performance, a topic which has received much less attention is the influence of tip clearance asymmetry or non-uniformity on compressor stability. Tip clearance asymmetry exists in all compressors to some extent, with the severity depending on both the mechanical design and machine operating condition.² A problem of interest is thus to determine how the stability of a multi-stage compressor is affected by the distribution of clearance around the annulus.

2.2 Approach: Description of Model

The compression system model is based on the conceptual framework described in [18] for examining effects of non-uniform inlet flow on compressor stability. A schematic is shown in Figure (2.1). There is a compressor which pumps flow to a plenum, which exhausts through an exit throttle. The flow external to the compressor is assumed inviscid and two-dimensional. The compressor and throttle are modeled as actuator disks, each of which has a nonlinear constitutive relation that includes a rudimentary description of blade row unsteady response.³ The compressor ducting is taken to be long enough so that there are no non-axisymmetric pressure field interactions

² In the context of this discussion tip clearance asymmetry will be considered to be a result of casing non-uniformity (stationary asymmetry) as opposed to variations in blade height (rotating asymmetry).

³ The details of the mathematical model used in this study are presented in Appendix A.

with the inlet and exit duct terminations. This is not a fundamental limitation of the model, but was done to (slightly) decrease algebraic complexity. Density changes in the plenum are assumed to be related to pressure changes through an isentropic relationship, and the inertia of the fluid in the throttle is neglected.

Stability analysis of a compression system generally consists of two distinct steps. The first step involves solution of the governing equations for the steady state background flow through the system. As is typical with hydrodynamic stability problems this solution can be obtained whether or not such a flow would be stable in practice. The second step involves adding a small perturbation to the background flow and determining from a (linearized) stability analysis whether or not such a disturbance grows or decays with time. The eigenvalues of the resulting system of linearized differential equations are the indications of stability.

In the model the uniform clearance compressor performance must be specified through pressure rise - mass flow characteristics. The characteristic utilized is the non-dimensional total-to-static pressure rise (ψ) as a function of flow coefficient (ϕ) where,

$$\psi = \frac{P_{out} - P_{t,in}}{\rho U^2} \quad \text{and} \quad \phi = \frac{V_x}{U} \quad (2.1)$$

It is through modification of this characteristic that the effects of clearance asymmetry are included.

For a compressor with circumferentially uniform tip clearance a single pressure rise characteristic is sufficient to represent the overall performance. For a compressor with asymmetric tip clearance, regions having smaller tip clearance produce increased pressure rise and those having larger clearance produce decreased pressure rise. The result will be a pressure rise that varies around the circumference and hence a non-axisymmetric axial velocity.

The approach taken here is to consider a compressor with asymmetric clearance as having different pressure rise characteristics at each circumferential location round the

annulus. (This is analogous to the parallel compressor concept which has been employed to study circumferential inlet distortion [17].) The peak pressure rise of these local characteristics depends upon the level of clearance at that location. Locally the pressure rise is assumed to follow the uniform clearance behavior: i.e. a 1% increase in clearance/chord produces approximately a 5% decrease in stalling pressure rise as shown in Figures (1.3a) and (1.3b).

A decrease in peak pressure rise capability is not all that results from an increase in clearance. Data also indicates that there is typically a change in stalling flow coefficient with the level of clearance; for a specific compressor the minimum stable flow coefficient is lower with smaller tip clearance. The model must thus account for observed changes in both pressure rise and in flow capacity.

It is useful to illustrate the procedure used to define the family of pressure rise characteristics which represent a compressor with asymmetric tip clearance. Figure (2.2) shows the total-to-static pressure rise characteristic, based on parameters for a three stage axial compressor, with uniform clearance equal to 3% of chord. This characteristic served as the nominal one for the computational study conducted here. Suppose a casing asymmetry is introduced in the form of a cosine shaped non-uniformity with amplitude equal to 2% of chord. The compressor will then have minimum and maximum clearance-to-chord of 1% and 5% respectively as shown in the schematic of Figure (2.3). Assume for the moment that clearance level affects only the peak pressure rise (and not the flow coefficient associated with the peak). If so, the peak pressure rise will vary around the annulus from 10% lower than nominal to 10% higher than nominal. The family of pressure rise characteristics for such a case is illustrated in Figure (2.4).⁴

As stated, the assumption of tip clearance only affecting pressure level is not general enough because most compressor data show that a change in clearance also affects the flow coefficient associated with the peak. For an asymmetric clearance

⁴ The mathematical formulation for the actual and isentropic compressor pressure rise characteristics used in this study is presented in Appendix B.

variation, the characteristics around the annulus would be expected to show variations in peak pressure rise and in flow coefficient at the peak. This behavior can be incorporated by shifting the peaks of the characteristics in a specified manner. Figure (2.5) shows characteristics for $\pm 2\%$ asymmetry using the same parameters as Figure (2.4) with the locus of peaks along a 45 degree line. The horizontal shift shown corresponds to a 38% change in flow coefficient from the highest to lowest characteristic peaks.

To incorporate effects associated with the unsteady viscous response of a blade row, the isentropic or lossless pressure rise characteristic for the compressor is required. Both the actual steady-state and the isentropic pressure rise characteristics must be provided for each circumferential location. The difference between the steady-state and isentropic pressure rise characteristics is the steady state loss. The isentropic characteristics are also dependent upon the local level of tip clearance (see Appendix B).

An important non-dimensional parameter which characterizes the system dynamic behavior is;

$$B = \frac{U}{2a} \sqrt{\frac{V_{plenum}}{AL_{total}}} \sim \frac{\text{Fluidic Compliance}}{\text{Fluidic Inertia}} \quad (2.2)$$

For a given compression system the value of B defines whether the mode of instability will be surge or rotating stall. Systems with B above a critical value exhibit surge oscillations, while those having B lower than this will undergo an initial transient to the quasi-steady flow and pressure rise associated with operation in rotating stall. In this investigation the effect of B on the system response was examined and will be discussed in Section (2.8). A more detailed discussion of the role of B in determining instability behavior is given in [2] and [4].

Scope of Calculations

A set of numerical simulations was conducted to determine the stability of a compression system with asymmetric tip clearance. The following calculations were executed:

- (1) **Baseline Compressor Stability Calculations (three-stage compressor)**
 - Effect of asymmetry magnitude on compressor instability point with characteristic peaks aligned.
 - For $\pm 2\%$ clearance asymmetry, effect of shifts in compressor characteristic peaks on instability onset.
 - (2) **Effect of Blade Row Unsteady Viscous Response on Baseline Results**
 - (3) **Effect of Compressor Characteristic Curvature**
 - Nominal characteristic with twice the curvature at the peak
 - Nominal characteristic with half the curvature at the peak
 - (4) **Effect of Compressor Peak Pressure Rise**
 - Characteristic with twice the baseline peak pressure rise (~ six-stages)
 - Characteristic with three times the baseline peak pressure rise (~ nine-stages)
 - (5) **Effect of Tip Clearance Asymmetry Distribution**
 - Continuous clearance variations of various wavelengths
 - Discrete or "notch like" clearance variations
- Cases (1) - (5) were run with B parameter of 0.05 in order to decouple the compressor dynamics from those of the system and thus ensure that a rotating stall mode would be the dominant instability [4].
- (6) **Effect of Compressor\Compression System Coupling on Baseline Results**
 - $\pm 2\%$ clearance asymmetry with characteristic peaks aligned
 - $\pm 2\%$ clearance asymmetry with characteristic peaks shifted along a 45 degree line

The reasons which underpin each of the choices will be discussed in subsequent sections, and the results of each of the investigations are detailed with an emphasis on the changes that tip clearance asymmetry introduces.

2.3 Baseline Compressor Stability Calculations

The initial set of calculations were conducted without inclusion of the blade row unsteady viscous response and with the peaks of the local pressure rise characteristics aligned. This was done to establish a baseline as well as to obtain some insight into the magnitude of the changes to be expected. A cosine clearance asymmetry was utilized with amplitudes varying from 0 to $\pm 2\%$ clearance/chord. (The pressure rise characteristic families for the uniform clearance and $\pm 2\%$ clearance variation cases are shown in Figures (2.2) and (2.4) respectively.)

Figures (2.6)-(2.12) illustrate the type of results obtained with compressor operating at neutral stability and having $\pm 2\%$ (of chord) clearance asymmetry. These are typical of those obtained with various levels of clearance non-uniformity. Table [2.1] lists the nominal values of the parameters used in the baseline calculations. The mathematical definitions for each of these variables is provided in Appendix A, as are the equations governing the background flow and stability.

Table [2.1]: System Parameters used in Baseline Simulations

Rotor fluid inertia, λ	0.68
Compressor fluid inertia, μ	1.01
Compressor inlet duct/radius	2
Compressor exit duct/radius	2
Nominal B - Parameter	0.05
Compressor degree of reaction, R	75%

In addition to the compressor characteristic slope, the inertia of the fluid in the compressor and rotor are linked to the compression system dynamics and hence the stability of the flow field to non-axisymmetric disturbances. The duct lengths are associated with the B - parameter and hence the mode of instability. The degree of reaction is utilized to determine the rotor-stator loss split when the unsteady viscous response model was included as described in Section (2.4).

Figures (2.6) and (2.7) show the time-mean background flow coefficient and pressure rise coefficient at the compressor face. The annulus is unwrapped and the coefficient values are given at each circumferential location. In this case the peaks of the local characteristics were aligned and the corresponding pressure rise round the annulus approximately follows the form of the cosine clearance geometry distribution. The average flow coefficient at neutral stability has increased from 0.5 (with no asymmetry) to 0.507, which is a 1.4% loss in flow range. There is also a decrease in peak pressure rise from 0.8 to 0.770, which corresponds to a 3.7% loss in pressure rise capability.

If the pressure rise and flow coefficient distributions given in Figures (2.6) and (2.7) are plotted together, a locus of steady state operating points around the annulus is obtained as illustrated in Figure (2.8). For clarity only the highest (smallest clearance), nominal, and lowest (largest clearance) compressor characteristics are shown. At neutral stability approximately half of the points around the annulus are operating on positively sloped portions of the compressor characteristic. The local characteristic slope for this locus is shown in Figure (2.9).

To determine the stability of the compression system, the eigenvalues of the governing linearized differential equations must be computed. Figure (2.10) shows these eigenvalues for the case illustrated in Figures (2.6) to (2.9). With the exception of the most highly damped eigenvalue, all the eigenvalues shown in Figure (2.10) are associated with rotating stall type modes for the compressor. The most damped eigenvalue located on the real axis is associated with plenum pressure perturbations. For

each eigenvalue there is a corresponding eigenvector (whose components are the Fourier coefficients of the perturbation) which gives the mode shape of the corresponding flow disturbance; these are the eigenmodes of the system. In Figure (2.10) the pair of eigenvalues associated with the first eigenmode are at neutral stability while the zeroth and higher eigenmodes remain damped. One can loosely view the zeroth eigenmode as a surge-like disturbance and the others as different order propagating stall like disturbances.

The first mode of the system is at neutral stability, and it is of interest to examine the corresponding mode shape. Figure (2.11) shows the unsteady flow coefficient perturbation at different times over a period versus circumferential position, illustrating the wave envelope for the mode. The wave changes shape as well as peak-to-peak amplitude while traveling around the annulus. The level of fluctuation that a stationary sensor, such as a hot wire, would see thus differs at different points round the annulus. The regions of wave growth and decay can be directly linked to those sections of the annulus where the compressor is locally operating on either the unstable (positive slope) or stable (negative slope) portion of the pressure rise characteristic family. Comparing the steady flow coefficient distribution of Figure (2.6) with the wave envelope in Figure (2.11) it is apparent that the region of reduced flow ($\phi < \text{nominal characteristic peak of } 0.5$) corresponds to wave amplification while the region with increased flow ($\phi > 0.5$) produces wave attenuation. The product of the pressure rise perturbation and mass flow perturbation, non-dimensionally $\delta\psi \cdot \delta\phi$ or $(\delta\phi^2) \cdot (\partial\psi/\partial\phi)$ is an indication of the unsteady energy input responsible for dynamic instability [5, 25]. Wave growth or decay in a particular portion of the annulus is therefore associated with the addition or dissipation of unsteady mechanical energy by the compressor in that region.

Figure (2.12) shows the harmonic content of the eigenmode in Figure (2.11). The clearance asymmetry introduces a non-uniformity in the background flow, so the eigenmodes of the system can have a rich harmonic content. The individual harmonic

magnitudes are constant since they represent the amplitudes of the temporally and spatially invariant Fourier coefficients. As expected the first harmonic is dominant, but the second and third harmonic amplitudes are also a significant fraction of the first.

For the case of inlet distortion, a criteria for compressor instability proposed by Hynes and Greitzer [18] and Chue et al [21] is that instability occurs when the integrated characteristic slope around the annulus is zero. The criteria was based upon the notion that a particular mode at neutral stability has one dominant harmonic. It does not hold when the instability mode has a spectral content which includes several harmonics with significant amplitudes. This is the case with tip clearance asymmetry, and thus the integrated mean slope instability criteria does not apply.

The results so far have been for a compressor with the peaks of the local pressure rise characteristics aligned. Now consider a $\pm 2\%$ tip clearance asymmetry with the peaks of the characteristic shifted so that they lie on a 45 degree line. (The compressor operating map for this configuration is shown in Figure (2.5).) The distortion introduced by clearance asymmetry has a more complex harmonic content, but the same trends are observed. Figure (2.13) illustrates the flow coefficient variation at the compressor face for an operating condition with the first mode of the system at neutral stability. In contrast to Figure (2.6), the distribution is no longer approximately sinusoidal and the corresponding pressure rise does not resemble the clearance geometry distribution. As shown in Figure (2.14) the locus of operating points around the annulus also encompasses a greater range of pressure rise and flow coefficient. All these effects can be attributed to the increased range of flow coefficients over which the characteristic peaks are now distributed. The average flow coefficient at neutral stability varies from 0.5 with no asymmetry to 0.531 with the $\pm 2\%$ clearance asymmetry and the peak shift.

The first mode wave envelope is also slightly different in shape than with the peaks aligned due to changes in local characteristic slope around the annulus, and the magnitude of the second harmonic has increased to approximately 80% of the first. The

eigenvalue structure is similar to that in Figure (2.10), but the frequency of the first mode is approximately 20% higher than with peaks aligned.

The most important effect of tip clearance asymmetry on compressor stability is the change in location of the neutral stability point. In Figure (2.15) the nominal pressure rise characteristic is shown along with the locus of neutral stability point movement for different levels of clearance asymmetry and peak shift. If tip clearance asymmetry is modeled as modulating peak pressure rise but not flow coefficient (i.e. local characteristic peaks remain aligned) the neutral stability point moves downward as shown in the first section (a) of the locus in Figure (2.15). An asymmetry amplitude of $\pm 2\%$ causes a 3.7% loss in peak pressure rise and a 1.4% increase in stalling flow coefficient.

To see the effect of characteristic peak alignment on neutral stability point location, the peaks were gradually moved from vertically aligned (Figure (2.4)) to aligned along a 45 degree line (Figure (2.5)). As the peaks were shifted horizontally, the neutral stability point was found to move to a higher flow coefficient and lower pressure rise, as illustrated in the lower section (b) of the locus in Figure (2.15). For $\pm 2\%$ clearance asymmetry the shift of the local characteristic peaks to a 45 degree line resulted in a 5.8% loss in peak pressure rise and 6.2% increase in stalling flow coefficient. Although the location of the neutral stability point depends upon the level of clearance asymmetry and the shape of the characteristic family, *all of the compressors examined had the same average tip clearance*. Thus, clearance asymmetry can produce a significant reduction in stall margin.

2.4 Effect of Blade Row Unsteady Viscous Response

The two-dimensional, incompressible stability model was also modified to include a simple model for the development of viscous losses within the compressor. The inclusion of this behavior tends to increase damping of the higher eigenmodes of the

system, increasing first mode dominance. This implies that the model will predict first mode stalling behavior, similar to that found experimentally (Paduano et al [24] and Haynes et al [26]).

The specific implementation is that unsteady total pressure losses in either the rotor or stator are modeled as first order lags, so the governing differential equation is,

$$\tau \frac{dL}{dt} = L_{steady\ state} - L \quad (2.3)$$

where the time constant τ is on the order of the blade row flow through time. The steady state loss in this equation is defined as the difference between the actual and isentropic pressure rise.

Since instantaneous total pressure losses now include time lags associated with the flow within the blade rows, the compressor pressure rise must respond accordingly. Consider an instantaneous reduction in flow coefficient for a compressor with uniform clearance operating on the positively sloped portion of the characteristic. Immediately after the flow reduction, the total pressure loss is still at its initial value, hence the actual pressure rise follows a path parallel to the isentropic pressure rise, which is negatively sloped. Therefore, the transient slope is more negative than the steady state slope, and the compressor is more stable than in steady state operation at the same mass flow. This has important implications for the inception of rotating stall since the stability of disturbances is dependent on the effective slope of the pressure rise characteristic [26].

To determine the impact of viscous response the baseline calculations were repeated for a compressors with design point efficiencies of 80% and 90% . (The design point was chosen to have 20% stall margin.) Figure (2.16) illustrates the locus of neutral stability points for the 90% efficient compressor with time constants (τ) of 1 and 1.5 times the average blade row flow-through time, as well as with quasi-steady losses. The results for the 80% efficient compressor are not shown since they differ by only 1-2% in pressure rise and flow coefficient from those obtained with 90% efficiency. Inclusion of

unsteady viscous response moves the location of the uniform clearance neutral stability point to the positively sloped section of characteristic. The choice of time constant is seen to produce less than a 1% change in the neutral stability flow coefficient. Figure (2.16) indicates that the qualitative movement of the neutral stability point with clearance asymmetry is essentially the same over the range of time constant examined. Quantitatively inclusion of unsteady response tends to slightly reduce the magnitude of the changes observed with clearance asymmetry. Because the differences are small, unless noted the calculations to be described have been conducted without unsteady viscous response.

2.5 Effect of Compressor Characteristic Curvature

Calculations have been conducted to assess how changes in radius of curvature at the peak of the pressure rise characteristic affect the neutral stability operating point. Generally, for the characteristics utilized in this study, altering the peak radius of curvature changes the compressor map width.

Three different levels of peak radius of curvature were examined: (i) a baseline case (ii) half the radius of the baseline case (iii) twice the radius of the baseline case. In all of the calculations the clearance asymmetry was cosinusoidal with amplitude between 0 and 2% of chord. Figure (2.17) illustrates the locus of neutral stability points for the three different peak curvature cases. As the peak radius of curvature is reduced the loss in stall margin increases for a given level of clearance asymmetry or peak shift, indicating that characteristics with sharper peaks have increased sensitivity to clearance asymmetry.

To understand why the sensitivity is increased, consider the baseline case shown in Figure (2.4). Calculation of the locus of operating points at neutral stability (Figure (2.8)) showed that approximately half the points around the annulus are in the unstable positive slope region of the compressor map. As the characteristic's radius of curvature

is reduced (sharper peaks), the variation in pressure rise and slope encountered around the annulus becomes greater for the same range of flow. Since regions of lower pressure rise and increased (steeper) positive slope are accessed by the compressor, this causes the onset of instability at a higher flow coefficient, thus reducing the stall margin.

2.6 Effect of Compressor Peak Pressure Rise

The baseline clearance asymmetry calculations were carried out for a three stage compressor with peak pressure rise of $\psi = 0.8$. To determine the effect of increasing the peak pressure rise, it is useful to think in terms of adding repeating stages to the three stage compressor model. To make a comparison where only pressure rise has been altered, the compressor map width was set to be the same regardless of the number of stages. For fixed map width increasing the peak height also results in a reduction of the peak radius of curvature. Figure (2.18) illustrates the pressure rise characteristics for the original three-stage compressor along with those for six and nine stage machines of the same map width. The highest, nominal, and lowest characteristics associated with a $\pm 2\%$ clearance asymmetry are shown for each of the machines.

Figure (2.19) gives the locus of neutral stability point movement for the three different map height cases. The results have been normalized by the peak quantities to allow direct comparison. As the maximum pressure rise increases, the loss in stall margin (pressure rise and flow) also increases for a given level of clearance asymmetry or peak shift. The reasons are analogous to those given for changes in peak curvature and hence will not be repeated here.

2.7 Effect of Tip Clearance Asymmetry Distribution

The role of the spatial distribution of tip clearance around the annulus has thus far not been investigated. To determine the impact of tip clearance geometry on stability, four different casing profiles were examined: (1) $\cos(\theta)$, (2) $\cos(2\theta)$, (3) $\cos(4\theta)$,

and (4) two 90 degree square notches (one above and one below the nominal clearance) separated by 90 degrees. The first three of these are continuous clearance variations which contain only a single spatial harmonic, while the fourth is a discrete clearance variation which, in theory, contains an infinite number of harmonics.

Because three of the clearance variations contain harmonics higher than the first, implying that unsteadiness can be more important, the unsteady viscous model was utilized. As suggested by Haynes et al [26], the time constant in the calculations was 1.5 times the average blade row flow-through time.

The locus of neutral stability points for each of the clearance geometries is shown in Figure (2.20).⁵ The clearance variations with the longest wavelength produced the greatest loss in stall margin. For the discrete notches the movement of the neutral stability point is similar to that of the cosine asymmetry because this non-uniformity has a dominant first harmonic. These trends are similar to those obtained concerning the spatial extent of circumferential inlet distortions; distortions with larger circumferential extent produced largest losses in stall margin.

One reason for the increased stability associated with shorter wavelength non-uniformities can be explained by analogy with one-dimensional unsteady flow in a duct. For a fixed amplitude stagnation pressure disturbance, as the reduced frequency increases, the amplitude of the velocity perturbation decreases. Similarly in the case of clearance asymmetry as the length of the non-uniform region decreases, the reduced frequency with respect to the non-uniformity increases. This decreases the amplitude of the axial velocity non-uniformity (a sort of "smoothing"), and hence the impact on stability. As an example, the background flow at neutral stability for the $\cos(2\theta)$ clearance variation is shown in Figure (2.21). The amplitude of the axial velocity non-uniformity was reduced to approximately half that obtained with the $\cos(\theta)$ asymmetry

⁵ Note that the magnitude of the asymmetry was varied between 0 and $\pm 2\%$ clearance/chord, and that the characteristic peaks were shifted to a maximum of 37 degrees from vertical. Peak shifts greater than this caused regions of flow reversal in the 9-stage case and made the numerical method diverge.

as shown in Figure (2.6). In summary, compressors having long wavelength (low reduced frequency) tip clearance asymmetry will experience more severe losses in stall margin than those having casing non-uniformity with short length scales.

2.8 Effect of Compressor\Compression System Coupling

The study so far has been aimed at examining the onset of instability as initiated by rotating stall like disturbances. To ensure this, all of the numerical simulations have been for compression systems which have very low B -parameter [4]. To investigate the effect of compressor-compression system coupling, the baseline computations with a cosine clearance asymmetry were repeated with B -parameters ranging from 0.05 to 0.8. The upper limit of 0.8 was chosen because B greater than this allowed the zeroth (“surge like”) mode to become unstable before the first (“stall like”) mode.

The impact of B - parameter on the zeroth and first eigenmode frequencies is illustrated in Figure (2.22) for the cases with uniform clearance and with $\pm 2\%$ clearance asymmetry with characteristic peaks aligned. For uniform clearance the frequency of the propagating disturbance scales with the rotor speed and is not affected by system parameters. However, the frequency of the surge like disturbance depends on the system dimensions and therefore B . With asymmetric clearance both the zeroth and first mode frequencies depend on B . In addition to the decrease in first mode frequency with B shown in Figure (2.22), there is also an associated change in the structure of the eigenmode. For the $\pm 2\%$ asymmetry case, Figure (2.23) gives the ratio of zeroth to first harmonic amplitude for the first mode, at neutral stability, as a function of B . As B is increased the zeroth harmonic (which is dominant in the zeroth surge like mode) begins to increase in amplitude.

To determine the impact on stability, it is useful to examine how the stalling pressure rise and flow coefficient change with B . Figures (2.24) and (2.25) give these results for $\pm 2\%$ asymmetry with the peaks of the characteristics aligned and shifted to 45

degrees. There is relatively little change in stalling pressure rise with B as shown in Figure (2.24), but Figure (2.25) indicates a larger variation in the stalling flow coefficient. This was expected since increasing B promotes larger mass flow excursions (i.e. lower flow coefficients are accessed) which have a greater effect on the average flow coefficient than on average pressure rise.

From Figures (2.24) and (2.25) there is a particular value of B for which the system demonstrates the greatest loss in stability. In these simulations this occurs at a B of approximately 0.4. Behavior similar to this was found by Chue et al [21] for inlet distortion. Chue et al [21] showed that for a particular value of B - parameter the zeroth and first harmonics will have a phase relationship which allows them to reinforce one another. Similarly, for non-uniform tip clearance this effect was responsible for the greater loss in stall margin at a particular B .

Experimental Investigation

Based on the model developed here, a set of experiments was designed to investigate the effects of tip clearance asymmetry on compressor performance and stability. These experiments were conducted by Wong [36] at the General Electric Co. (GE) Aerodynamic Research Laboratory using a low-speed four-stage axial compressor. The experiments will be reported in detail [36].

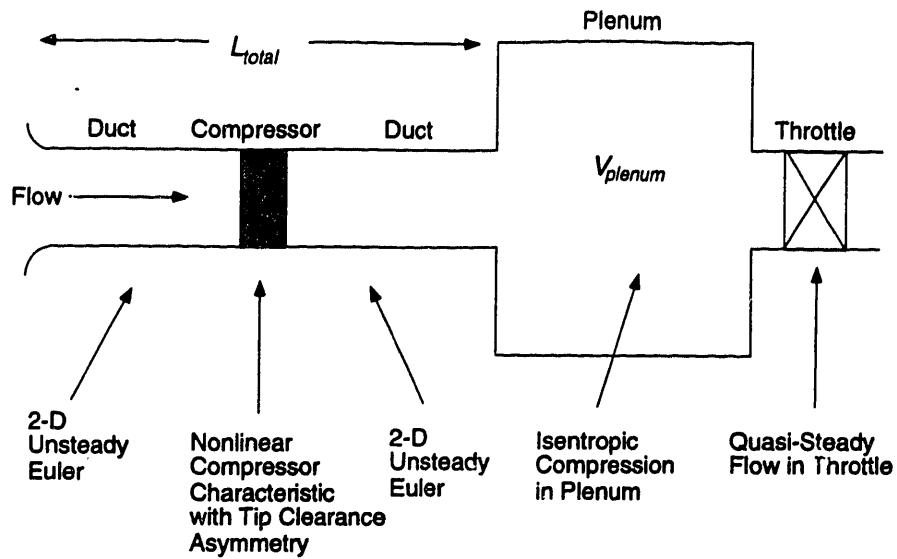


Figure (2.1): Schematic of compression system used for stability model

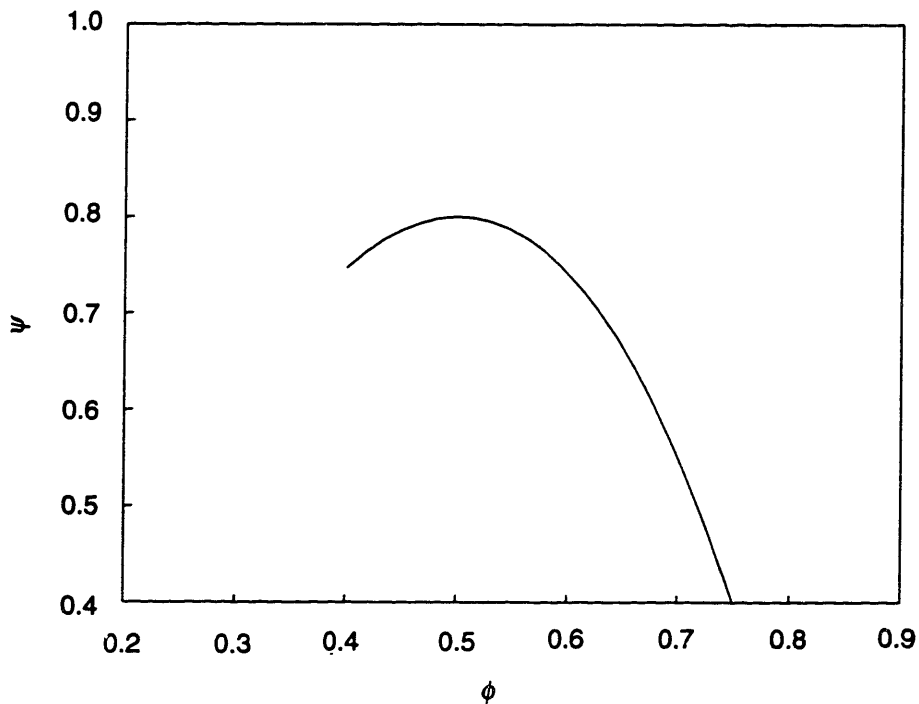


Figure (2.2): Baseline three-stage compressor pressure rise characteristic

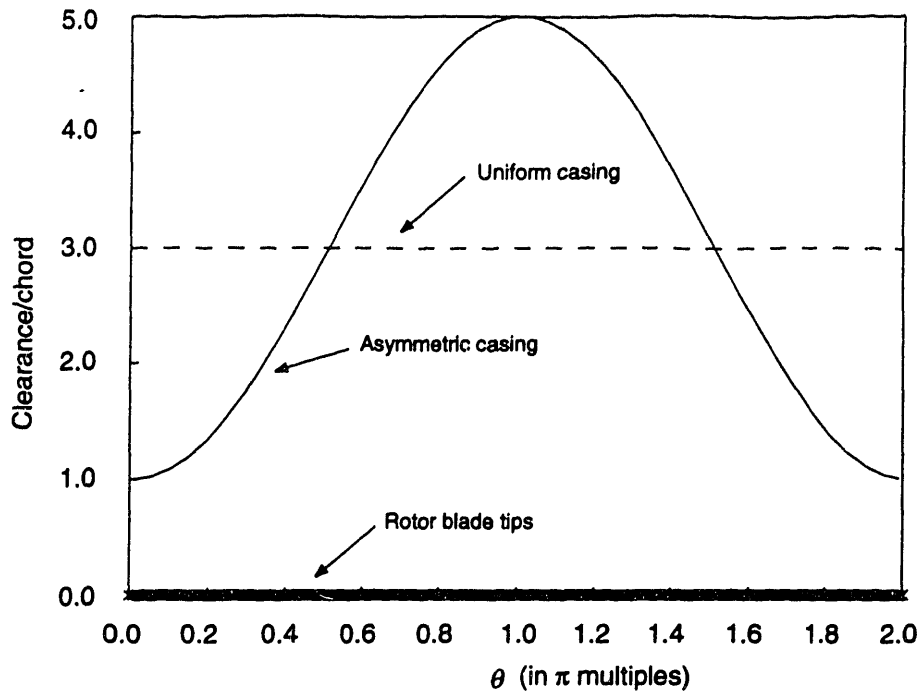


Figure (2.3): Tip clearance distributions with uniform casing and 2% of chord cosine shaped asymmetry

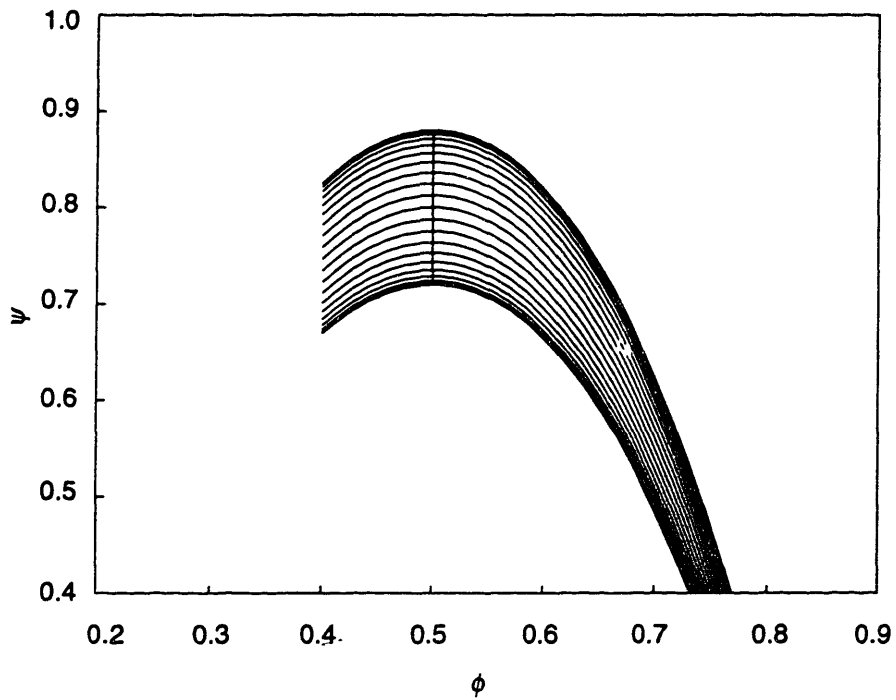


Figure (2.4): Three-stage compressor characteristic family for 2% clearance asymmetry with peaks aligned

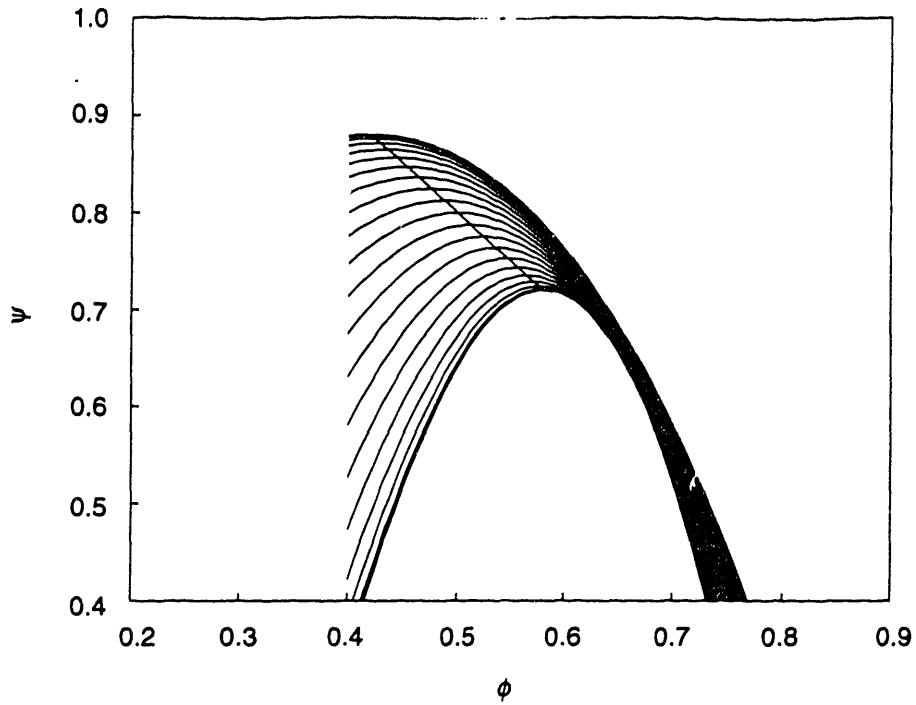


Figure (2.5): Three-stage compressor characteristic family for 2% clearance asymmetry with peaks along a 45 degree line

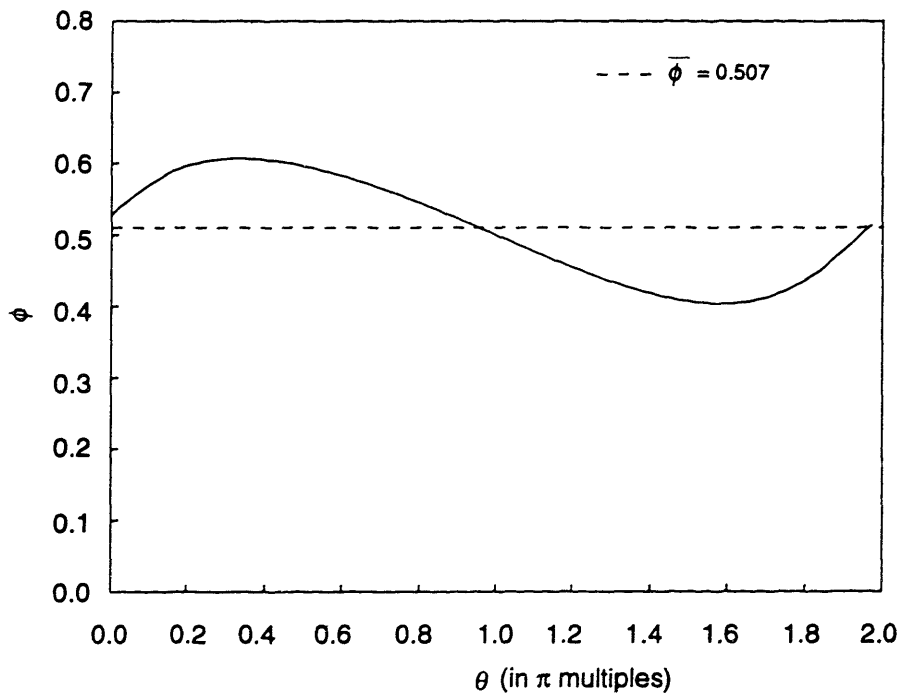


Figure (2.6): Flow coefficient distribution at compressor face at neutral stability for 2% cosine clearance asymmetry with characteristic peaks aligned

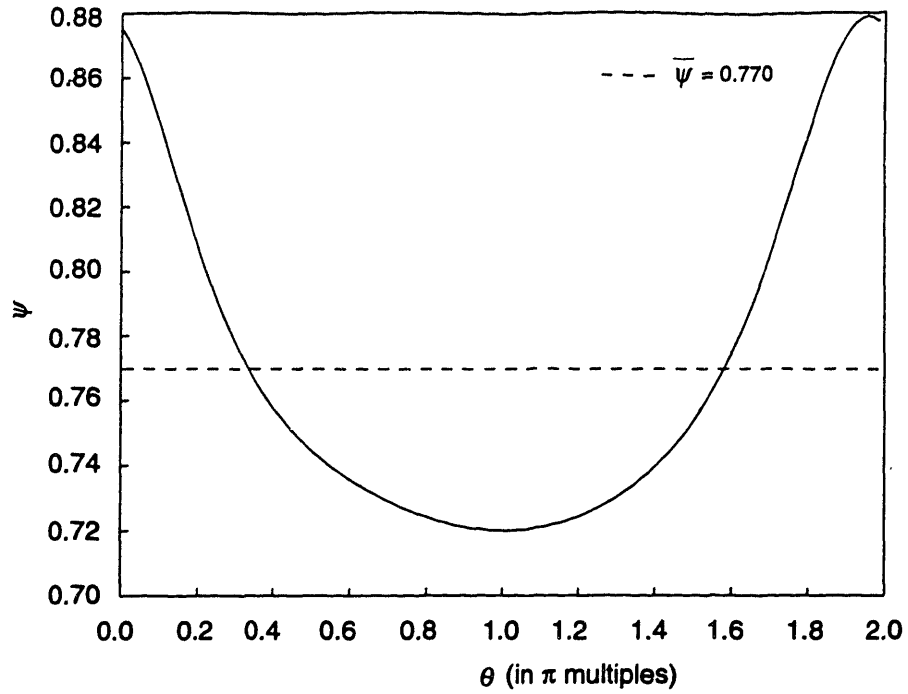


Figure (2.7): Pressure rise coefficient distribution at compressor face at neutral stability for 2% cosine clearance asymmetry with characteristic peaks aligned

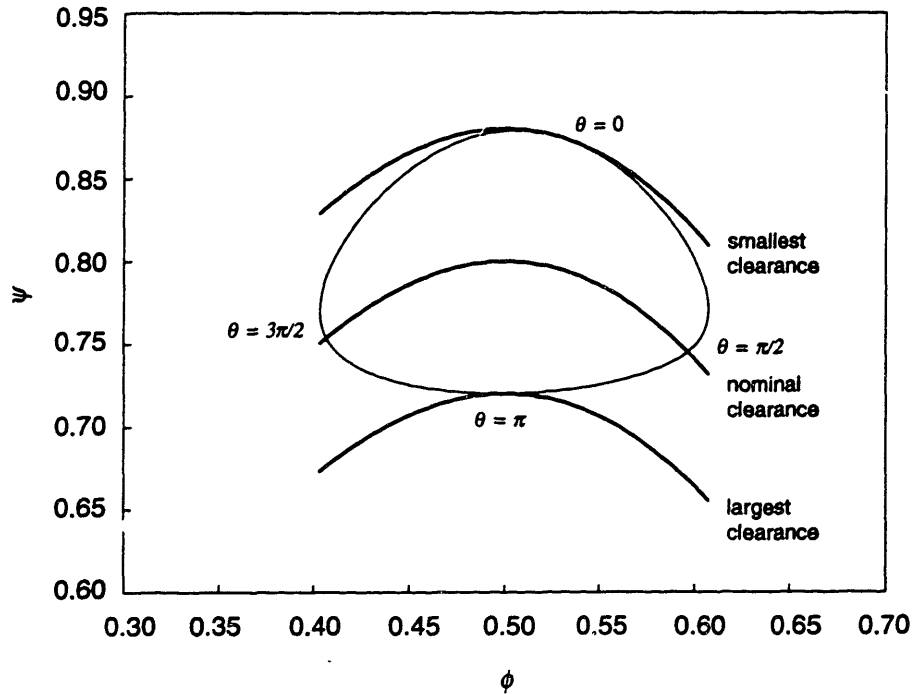


Figure (2.8): Locus of operating points around annulus at neutral stability

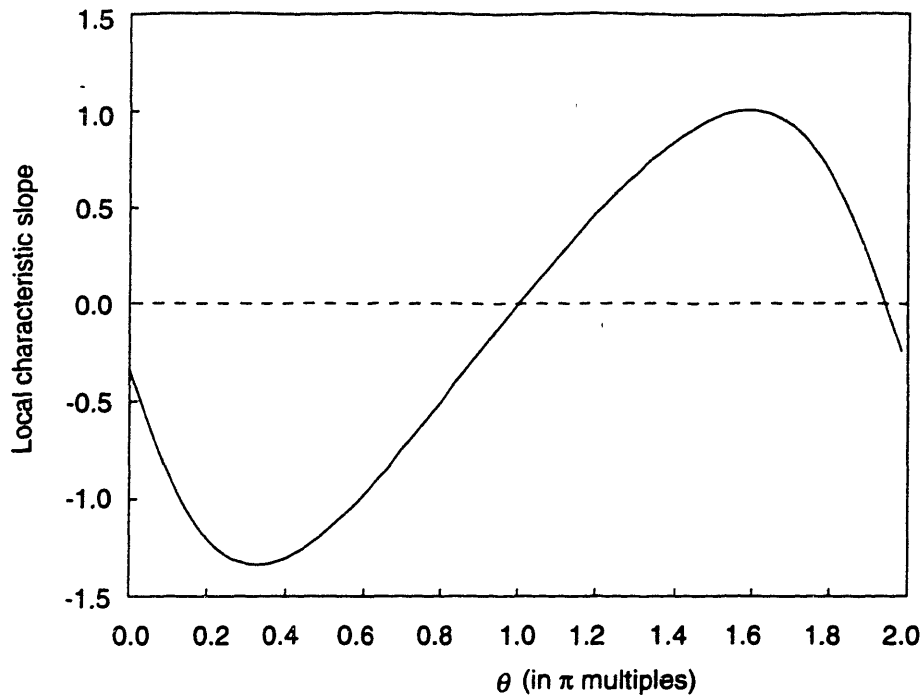


Figure (2.9): Pressure rise characteristic slope variation at neutral stability for 2% cosine clearance asymmetry with characteristic peaks aligned

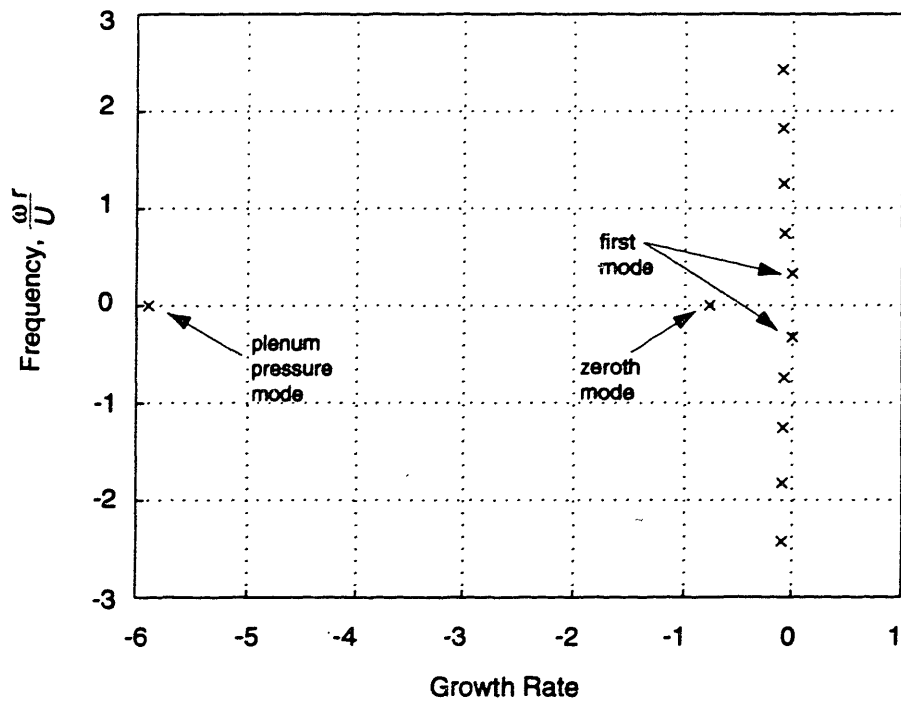


Figure (2.10): Compression system eigenvalues at neutral stability

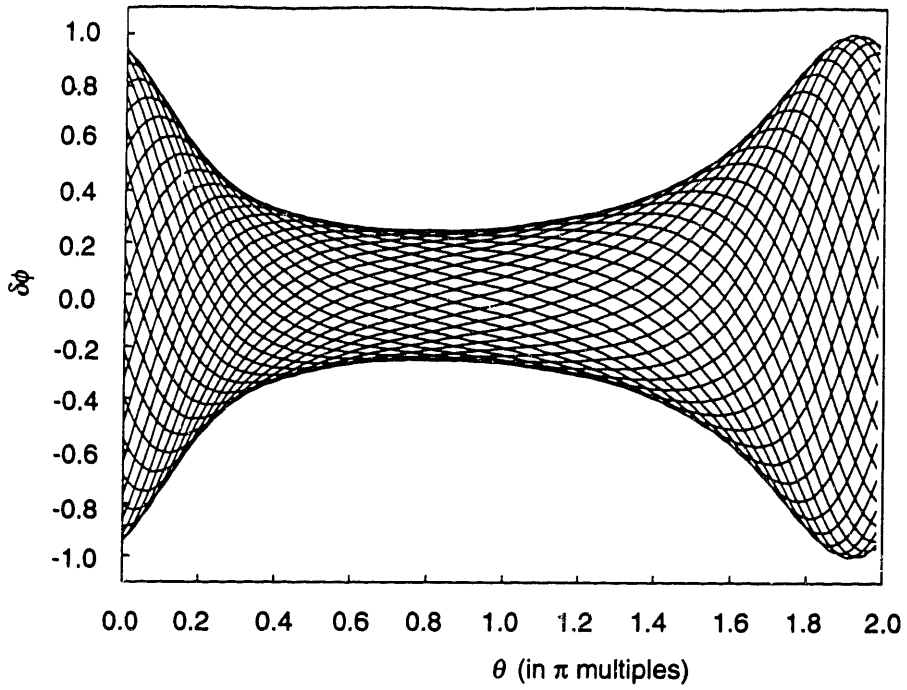


Figure (2.11): First mode wave envelope (flow coefficient perturbation) at neutral stability

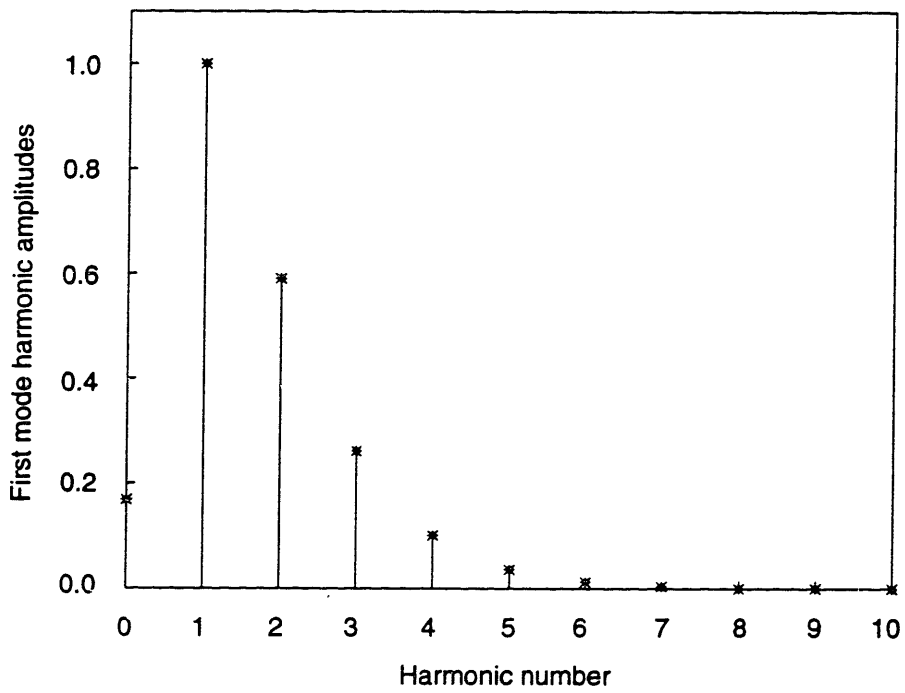


Figure (2.12): Spectral content of first mode at neutral stability

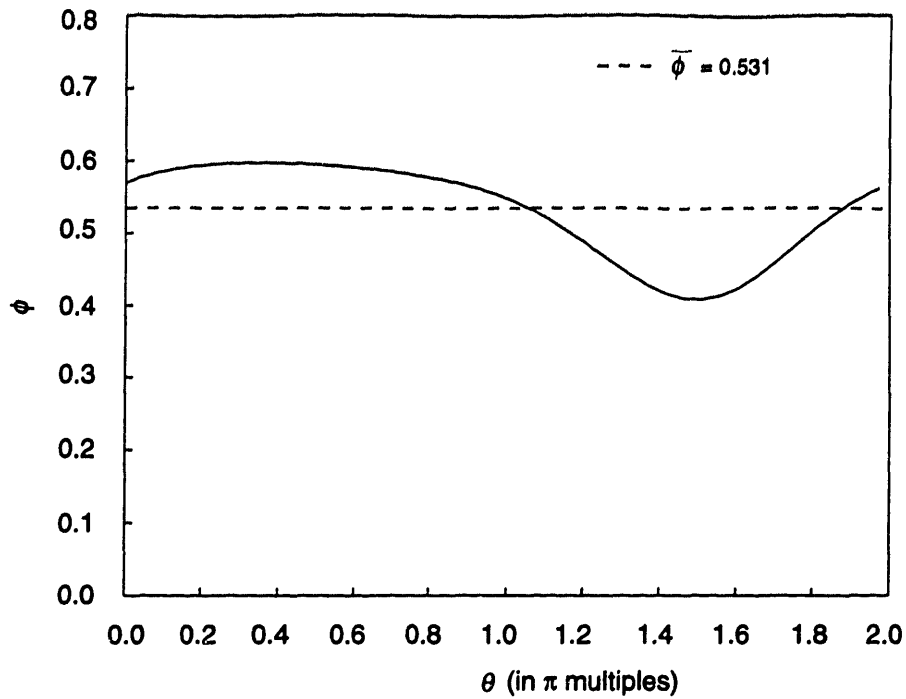


Figure (2.13): Flow coefficient distribution at compressor face at neutral stability for 2% cosine clearance asymmetry with characteristic peaks along a 45 degree line

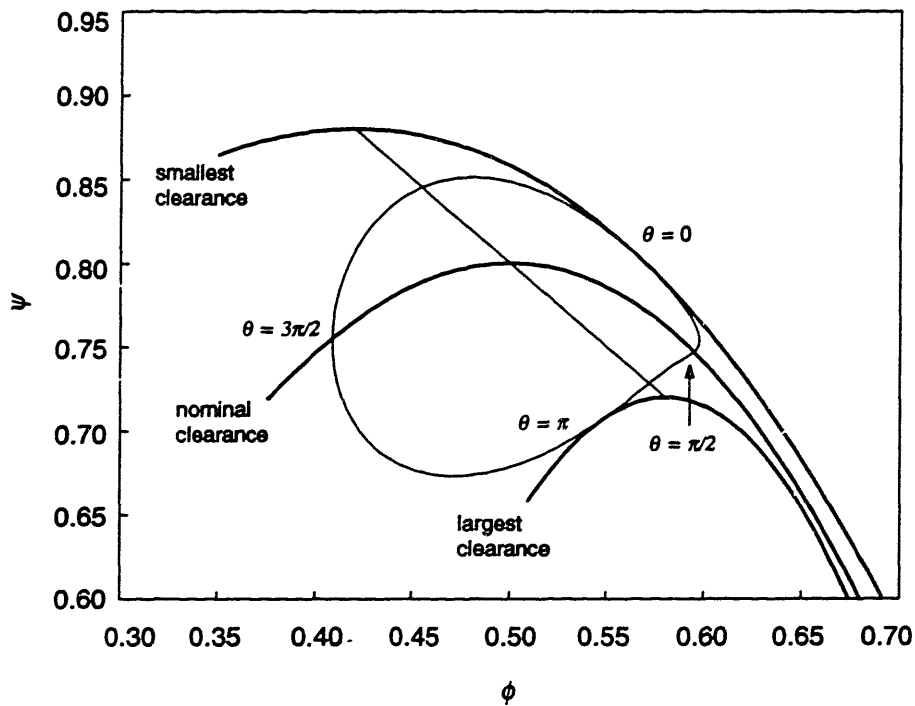


Figure (2.14): Locus of operating points around annulus at neutral stability with characteristic peaks along a 45 degree line

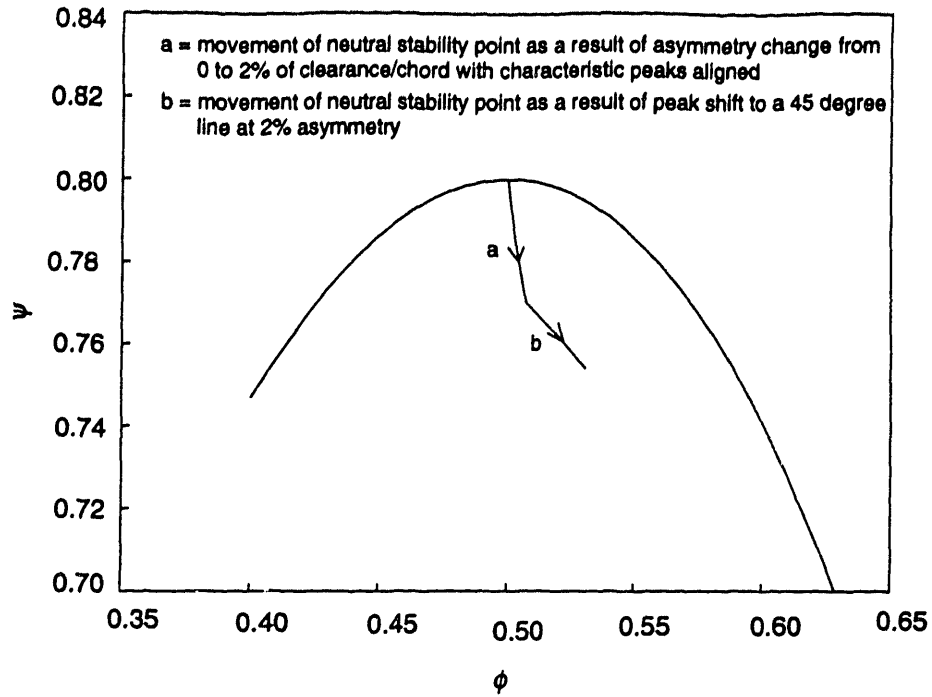


Figure (2.15): Locus of neutral stability point movement with cosine clearance variation

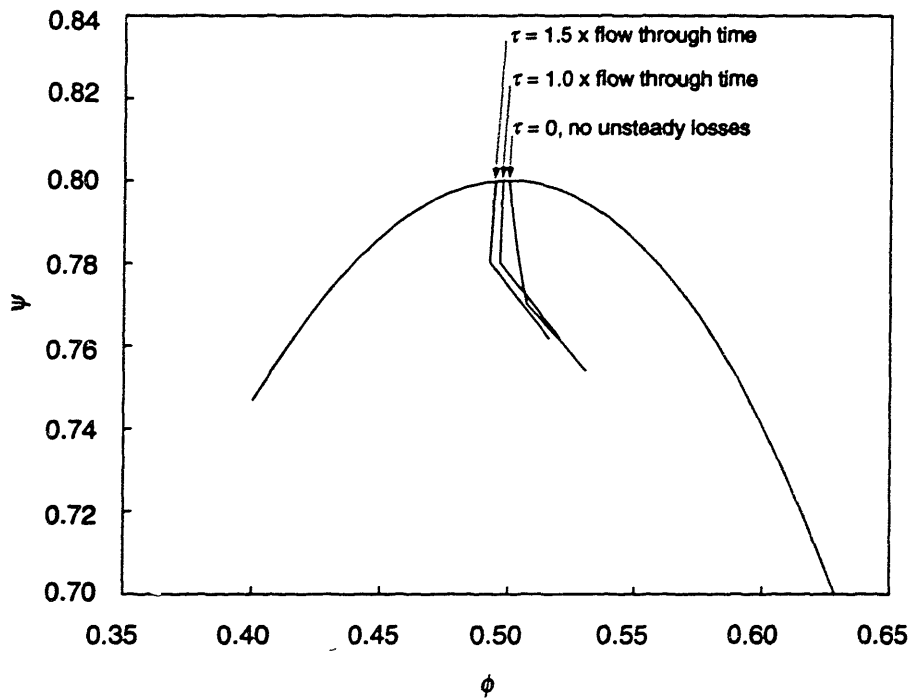


Figure (2.16): Effect of unsteady viscous response on neutral stability point movement with cosine clearance variation and characteristic peak shift

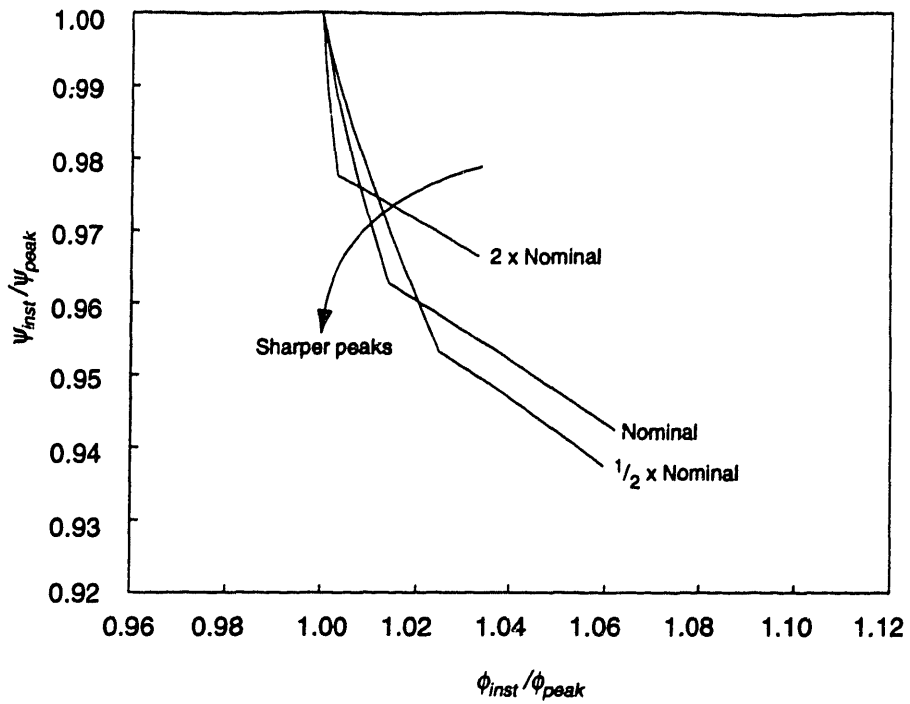


Figure (2.17): Effect of characteristic peak curvature on neutral stability point movement with cosine clearance variation and characteristic peak shift

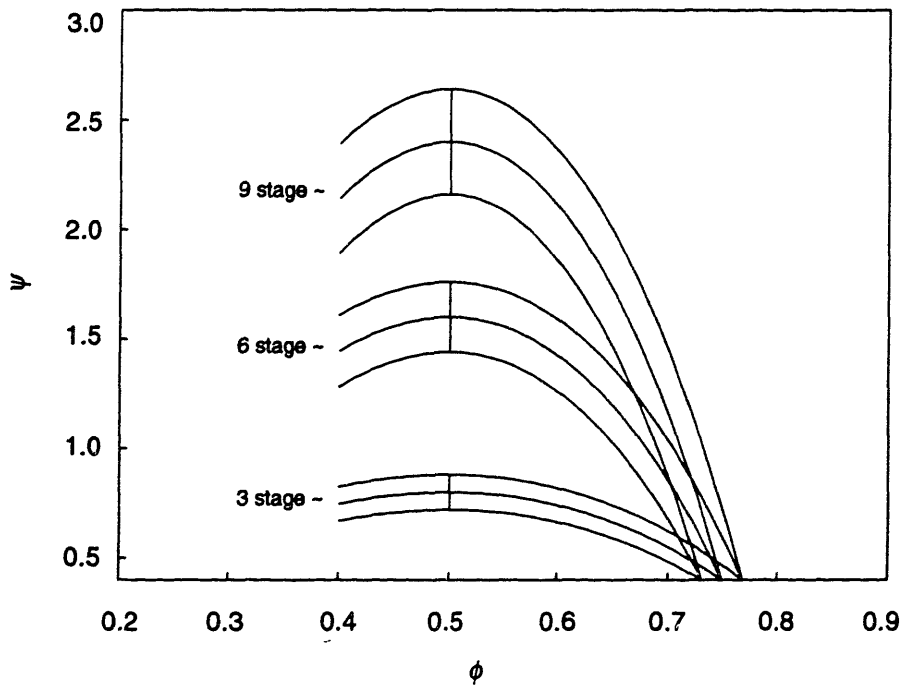


Figure (2.18): Characteristic families of differing peak pressure rise

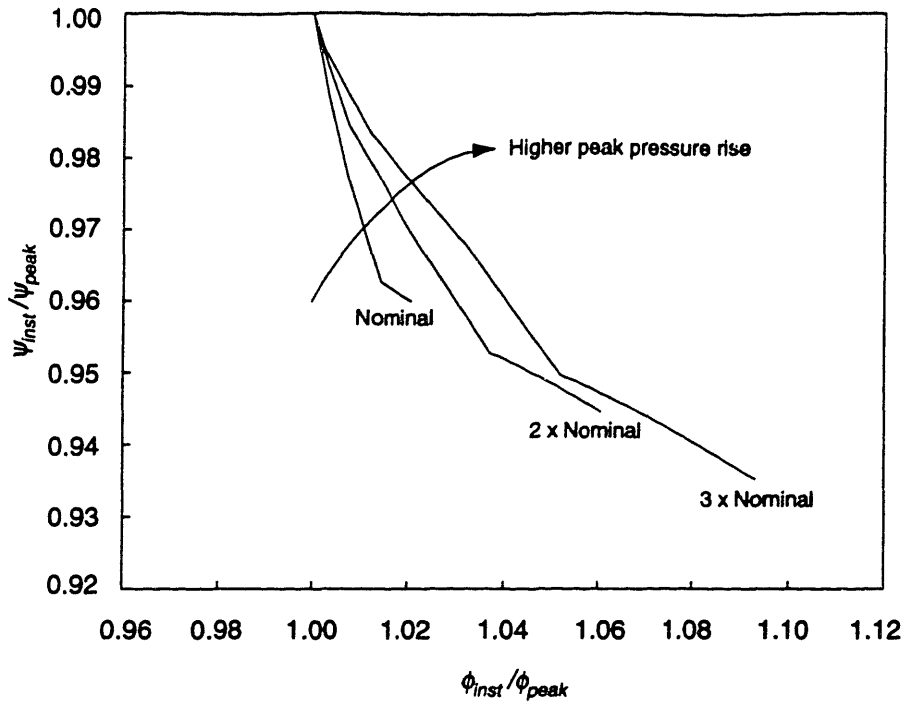


Figure (2.19): Effect of compressor peak pressure rise on neutral stability point movement with cosine clearance variation and characteristic peak shift

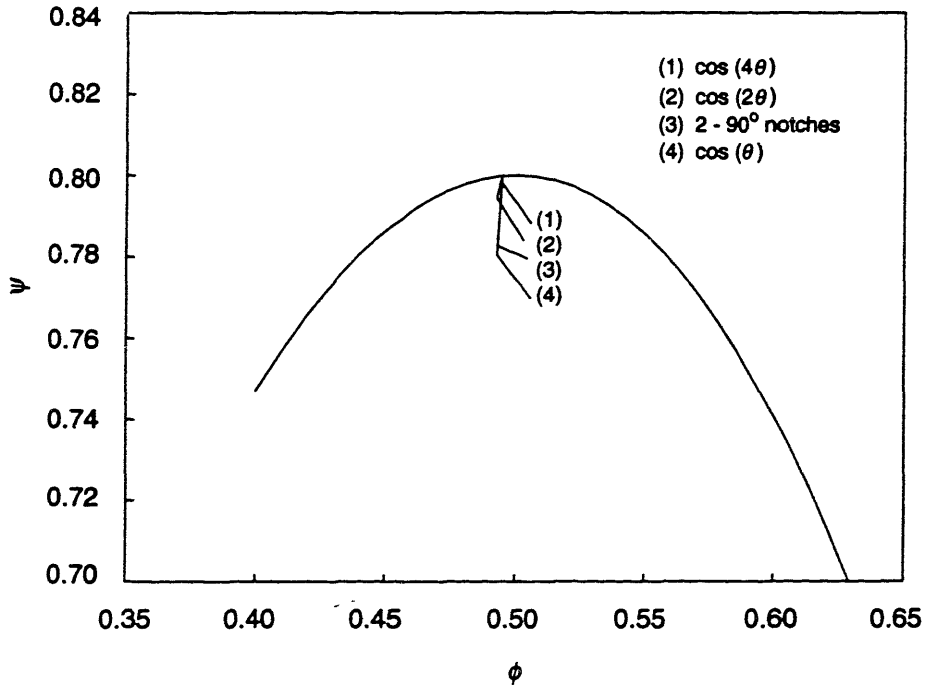


Figure (2.20): Effect of tip clearance distribution on neutral stability point movement (computed with unsteady viscous response)

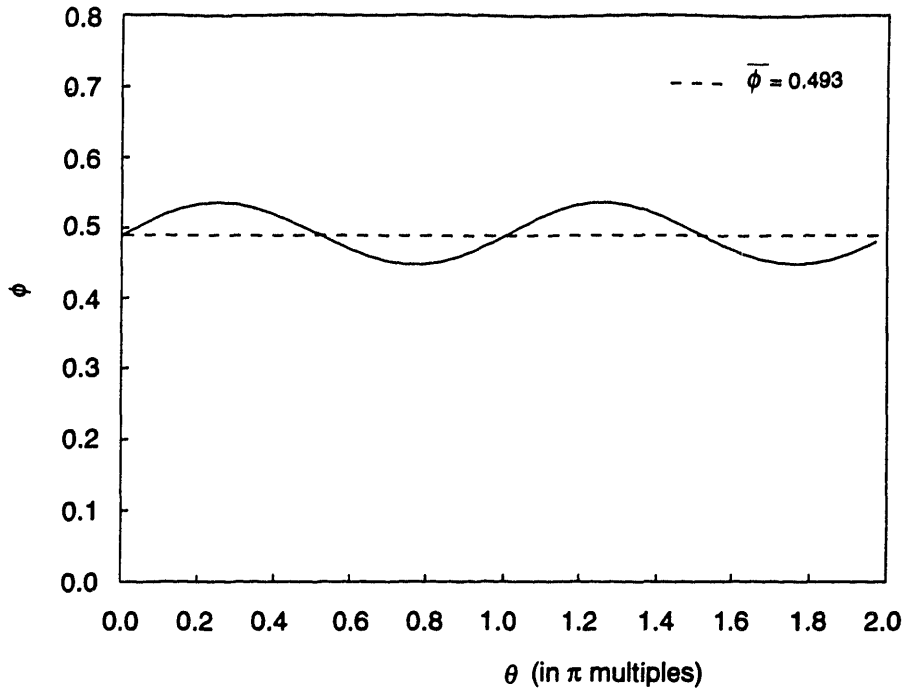


Figure (2.21): Flow coefficient distribution at compressor face at neutral stability for 2% of chord $\cos(2\theta)$ clearance asymmetry with characteristic peaks aligned

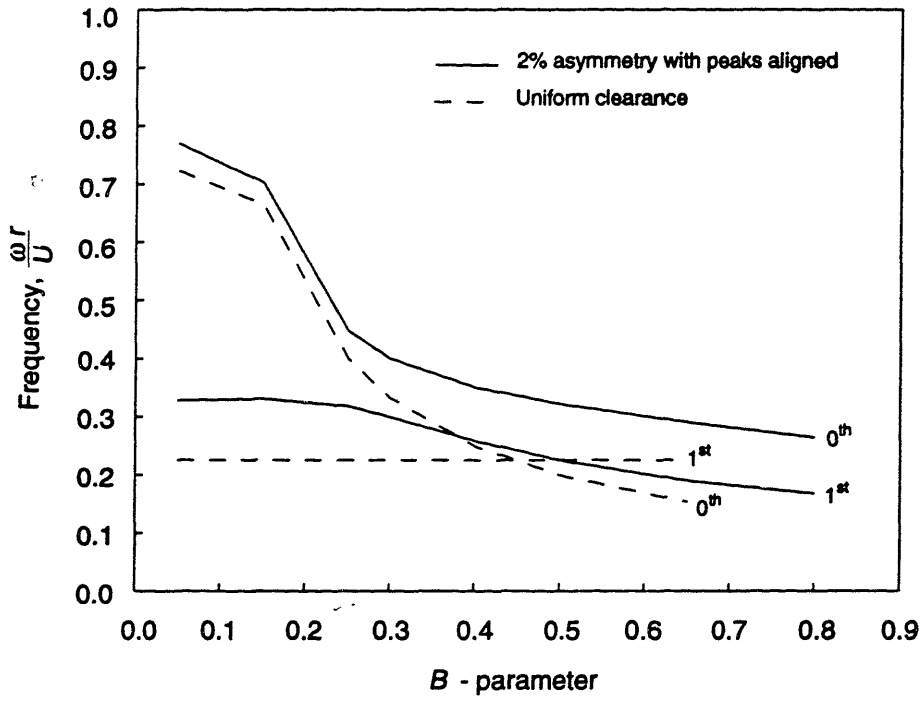


Figure (2.22): Zeroth and first mode frequencies with and without clearance asymmetry

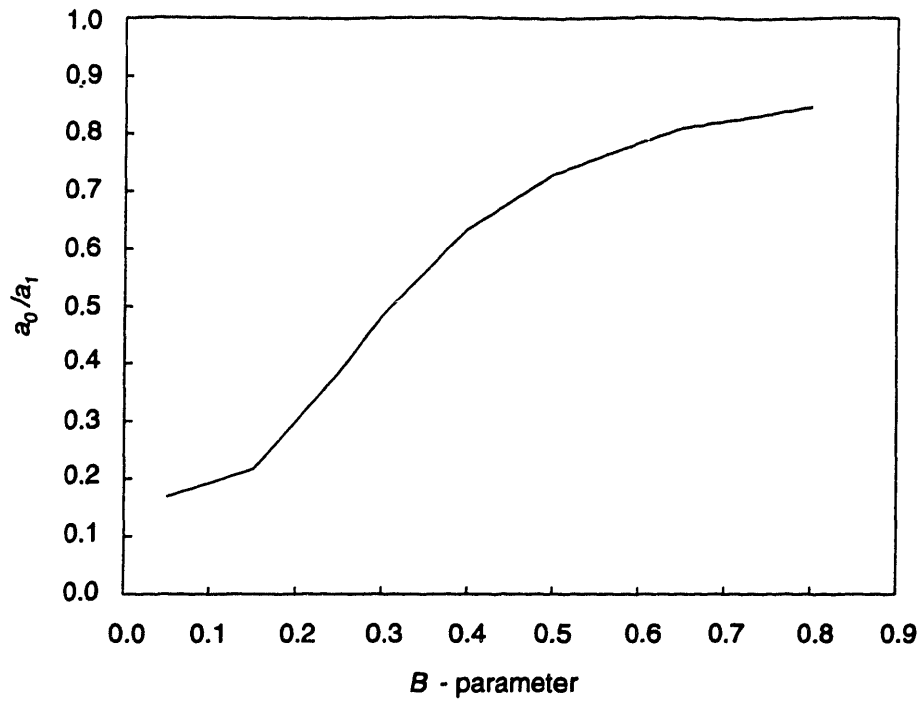


Figure (2.23): Ratio of Fourier components of first eigenmode at neutral stability with cosine clearance variation with characteristic peaks aligned

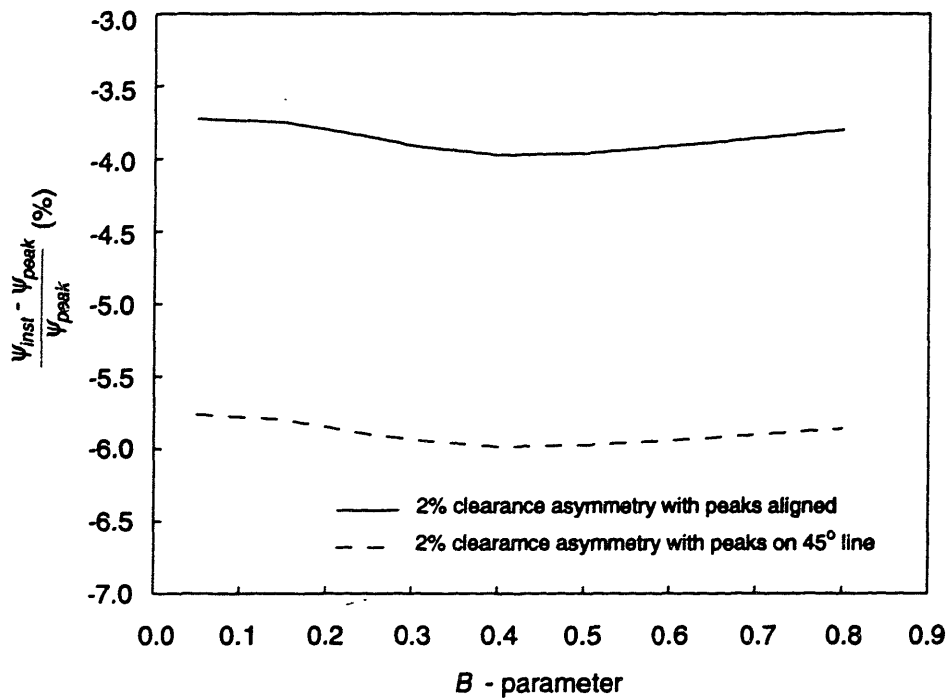


Figure (2.24): Loss in peak pressure rise capability with B - parameter

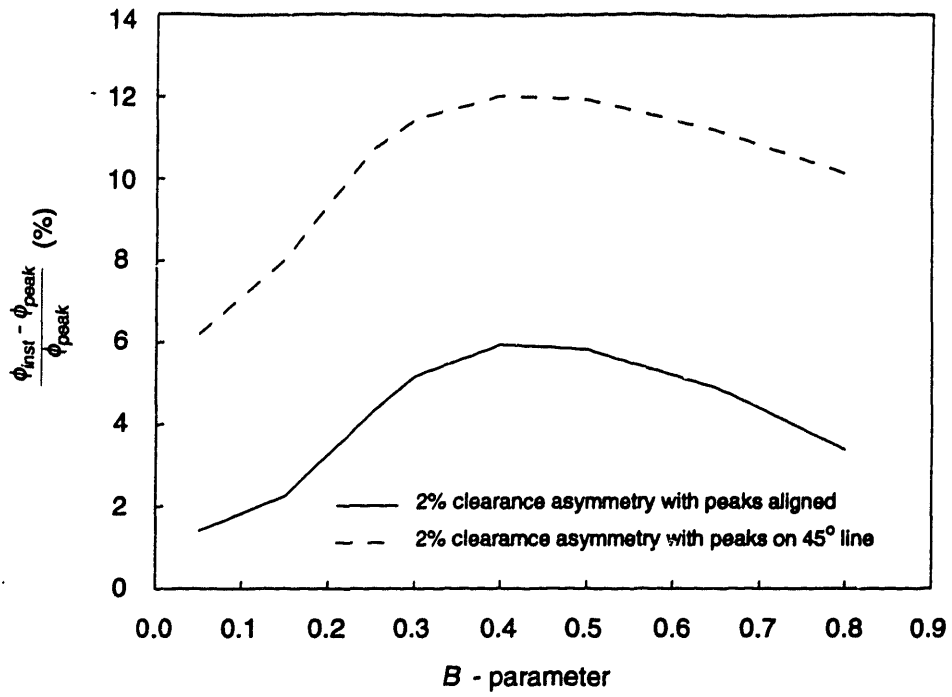


Figure (2.25): Change in flow coefficient at instability with B - parameter

Conclusions

3.1 Summary and Conclusions

The effect of tip clearance asymmetry on compressor stability has been studied using a two-dimensional, incompressible, stability analysis. Multi-stage compressor experiments with asymmetric clearance have been designed using this new model [36]. In the model the tip clearance asymmetry was analysed by viewing each circumferential location as operating on a different pressure rise characteristic corresponding to the local level of clearance.

The results of the computations carried out were:

- Increasing the magnitude of the clearance asymmetry decreased the stalling pressure rise and increased the stalling flow coefficient. The loss in pressure rise capability was generally closer to that based on the maximum clearance.
- Decreasing the wavelength of the clearance non-uniformity (i.e. increasing the reduced frequency) decreases the effect of clearance asymmetry on stall margin.
- Compressor characteristics which are steep, have high peak pressure rise, narrow map width, and sharp drop in pressure rise after the peak, promote sensitivity to clearance asymmetry.
- For a given compressor, sensitivity to clearance asymmetry is a weak function of B -parameter.
- Distortions generated by tip clearance asymmetry have a rich harmonic content and do not satisfy the integrated mean slope criteria for instability onset.

3.2 Implications of Present Work

The results of this study suggest one possibility for modifying compressor designs to improve tolerance to tip clearance asymmetry. For a particular machine having a fixed amplitude casing non-uniformity (e.g. $\pm 2\%$ of chord), the loss in stall margin was found to reduce as the wavelength of the asymmetry was shortened. To decrease the sensitivity to clearance asymmetry one can increase the number of circumferential casing segments. The present investigation indicates that essentially all the benefits are obtained when 4 or more casing segments are employed.

3.3 Recommendations for Future Work

The following list summarizes some directions in which the present study could be extended or enhanced.

- A study of the stall inception process with clearance asymmetry may be of interest to determine if the pre-stall disturbance structure is influenced. Two specific questions are whether the initial disturbances are two- or three-dimensional in nature and is this important when characterizing the effects of asymmetry on the overall system?
- The impact of clearance asymmetry on high speed compressor stability should be examined to determine if the effects are more severe in that flow environment.
- Using a framework similar to that employed in the present study, the effects of rotating asymmetry on compressor stability and performance can be examined.

References and Bibliography

- [1] Greitzer, E. M., "Review: Axial compressor stall phenomenon," *ASME J. Fluids Eng.*, 1980, vol. 102, 134-151.
- [2] Greitzer, E. M., "The stability of pumping systems - The 1980 Freeman Scholar Lecture," *ASME J. Fluids Eng.*, 1981, vol. 103, 193-242.
- [3] Emmons, H. W., Pearson, C. E., Grant, H. P., "Compressor surge and stall propagation," *Trans. ASME*, 1955, vol. 77, 455-469.
- [4] Greitzer, E. M., "Surge and rotating stall in axial flow compressors, Part I: Theoretical compression system model," *ASME J. Eng. Power*, 1976, vol. 99, 190-198.
- [5] Greitzer, E. M., "Surge and rotating stall in axial flow compressors, Part II: Experimental results and comparisons with theory," *ASME J. Eng. Power*, 1976, vol. 99, 199-217.
- [6] Smith, L. H., Jr., "The effect of tip clearance on the peak pressure rise of axial-flow fans and compressors," *ASME Symposium on Stall*, 1958, 149-152.
- [7] Baghdadi, S., "Modeling tip clearance effects in multi-stage axial compressors," *ASME Paper*, 95-GT-291, 1995.
- [8] Koch, C. C., "Stalling pressure rise capability of axial flow compressor stages," *ASME J. Eng. Power*, 1981, vol. 103, 645-656.
- [9] Wisler, D. C., "Loss reduction in axial-flow compressors through low-speed model testing," *ASME J. Eng. Gas Turbines and Power*, 1985, vol. 107, 354-363.
- [10] Smith, G. D. J., Cumpsty, N. A., "Flow phenomena in compressor casing treatment," *ASME J. Eng. Gas Turbines and Power*, 1984, vol. 106, 532-541.
- [11] McDougall, N. M., Cumpsty, N. A., Hynes, T. P., "Stall inception in axial compressors," *ASME J. Turbomachinery*, 1990, vol. 112, 116-125.
- [12] Goto, A., "Three-dimensional flow and mixing in an axial flow compressor with different rotor tip clearances," *ASME Paper*, 91-GT-89, 1991.
- [13] Wisler, D. C., "Advanced compressor and fan systems," General Electric Aircraft Engine Business Group Publication, Cincinnati, Ohio, 1985.
- [14] Moore, F. K., "A theory of rotating stall multistage axial compressors: Parts 1-3," *ASME J. Eng. Power*, 1984, vol. 106, 313-336.

- [15] Moore, F. K., Greitzer, E. M., "A theory of post stall transients in axial compression systems: Part I - Development of equations," *ASME J. Eng. Gas Turbines and Power*, 1986, vol. 108, 68-76.
- [16] Greitzer, E. M., Moore, F. K., "A theory of post stall transients in axial compression systems: Part II - Application," *ASME J. Eng. Gas Turbines and Power*, 1986, vol. 108, 231-239.
- [17] Mazzawy, R. S., "Multiple segment parallel compressor model for circumferential flow distortion," *ASME J. Eng. Power*, 1977, vol. 99, 228-246.
- [18] Hynes, T. P., Greitzer, E. M., "A method for assessing effects of inlet flow distortion on compressor stability," *ASME J. Turbomachinery*, 1987, vol. 109, 371-379.
- [19] Longley, J. P., "Measured and predicted effects of inlet distortion on axial compressors," ASME Paper, 90-GT-214, 1990.
- [20] Strang, E. J., "Influence of unsteady losses and deviation on compression system stability with inlet distortion," Master's Thesis, Massachusetts Institute of Technology, Department of Aeronautics and Astronautics, 1991.
- [21] Chue, R., Hynes, T. P., Greitzer, E. M., Tan, C. S., Longley, J. P., "Calculations of inlet distortion induced compressor flow field instability," *Int. J. Heat and Fluid Flow*, 1989, vol. 10, 211-223.
- [22] Longley, J. P., "A review of non-steady flow models for compressor stability," ASME Paper, 93-GT-17, 1993.
- [23] Garnier, V. H., Epstein, A. H., Greitzer, E. M., "Rotating waves as a stall inception indication in axial compressors," *ASME J. Turbomachinery*, 1991, vol. 113, 290-301.
- [24] Paduano, J. D., Epstein, A. H., Valavani, L., Longley, J. P., Greitzer, E. M., Guenette, G. R., "Active control of rotating stall in a low speed axial compressor," *ASME J. Turbomachinery*, 1991, vol. 115, 48-56.
- [25] Gysling, D. L., Greitzer, E. M., "Dynamic control of rotating stall in axial flow compressors using aeromechanical feedback," *ASME J. Turbomachinery*, 1995, vol. 117, 307-319.
- [26] Haynes, J. M., Hendricks, G. J., Epstein, A. H., "Active stabilization of rotating stall in a three-stage axial compressor," *ASME J. Turbomachinery*, 1994, vol. 116, 226-239.
- [27] Longley, J. P., Shin, H. -W., Plumley, R. E., Silkowski, P. D., Day, I. J., Greitzer, E. M., Tan, C. S., Wisler, D. C., "Effects of rotating inlet distortion on multistage compressor stability," ASME Paper 94-GT-220, 1994.
- [28] Tryfonidis, M., Etchevers, O., Paduano, J. D., Epstein, A. H., Hendricks, G. J., "Prestall behavior of several high-speed compressors," *ASME J. Turbomachinery*, 1995, vol. 117, 62-80.

- [29] Day, I. J., "Stall inception in axial flow compressors," *ASME J. Turbomachinery*, 1993, vol. 115, 1-9.
- [30] Horlock, J. H., Greitzer, E. M., "Non-uniform flows in axial compressors due to tip clearance variation," *IMEchE, Proc. Instn. Mech. Engrs*, 1983, vol. 197C, 173-178.
- [31] Colding-Jorgensen, J., "Prediction of rotor dynamic destabilizing forces in axial flow compressors," *ASME J. Fluids Eng.*, 1992, vol. 114, 621-625.
- [32] Ehrich, F., "Rotor whirl forces induced by the tip clearance effect in axial flow compressors," *ASME J. Vibration and Acoustics*, vol. 115, 509-515.
- [33] Epstein, A. H., Ffowcs Williams, J. E., Greitzer, E. M., "Active suppression of aerodynamic instabilities in turbomachines," *AIAA J. Propulsion and Power*, vol. 5, 204-211.
- [34] Paduano, J. D., Greitzer, E. M., Epstein, A. H., Guenette, G. R., Gysling, D. L., Haynes, J., Hendricks, G. J., Simon, J. S., Valavani, L., "Smart engines: Concept and application," *Integrated Computer-Aided Engineering*, 1993, vol. 1, 3-28.
- [35] Smith, L. H., Jr., "Casing boundary layers in multistage axial flow compressors," in *Flow Research on Blading*, edited by L. S. Dzung, Elsevier Publishing Co., 1970.
- [36] Wong, T. S., "Effects of Asymmetric tip clearance on compressor performance and stability," Master's Thesis, Massachusetts Institute of Technology, Department of Aeronautics and Astronautics, 1996.
- [37] Van Schalkwyk, C. M., "Active control of rotating stall with inlet distortion," Doctoral Thesis, Massachusetts Institute of Technology, Department of Aeronautics and Astronautics, 1996.

Appendix A

Equations in Compression System Stability Model

The equations described in this appendix were utilized to determine both the background steady flow and the hydrodynamic stability of this flow to small (linearized) disturbances. For additional details regarding the development of the equations given here, the work of Moore and Greitzer [15], Hynes and Greitzer [18], Longley [22], and Haynes et al [26] are good references.

The compression system to be modeled is that shown in the schematic of Figure (2.1). The assumptions utilized to develop the mathematical model are as follows:

Assumptions:

- Inlet conditions to system are uniform and constant
- Two-dimensional, inviscid flow in all ducts
- Compressor and throttle are represented as actuator disks
- Pressure rise across compressor is modified by pressure difference required to overcome the inertia of fluid within the blade rows
- Compressor outflow is axial
- Static pressure in the plenum is determined by exit throttle setting
- Flow in the plenum is spatially uniform and isentropic
- Pressure drop through throttle is quasi-steady with the time-averaged, annulus averaged flow coefficient.

A.1 Steady Background Flow

For steady flow in the compression system shown in Figure (2.1), the following relations hold.

Upstream Duct:

$$P_{i1}(\theta) = P_{i2}(\theta) \quad (\text{A1})$$

Compressor:

$$\frac{P_3 - P_{i2}}{\rho U^2} = \psi_i - L_r - L_s - \lambda \frac{\partial \phi}{\partial \theta} \quad (\text{A2})$$

$$T = \frac{b_x}{U \cos^2 \gamma}$$

$$\lambda = \sum_{i=1}^N \frac{U}{r} (T_{r,i}) \quad (\text{A3})$$

The rotor and stator loss are determined using the reaction distribution,

$$L_s = (1 - R)(\psi_i - \psi) \quad (\text{A4})$$

$$L_r = R(\psi_i - \psi) \quad (\text{A5})$$

Downstream Duct/Plenum:

$$P_3(\theta) = P_4(\theta) \quad (\text{A6})$$

Throttle:

$$\frac{P_4 - P_5}{\rho U^2} = \frac{1}{2} k_t \bar{\phi}_3^2 \quad (\text{A7})$$

The mathematical and physical description of ψ and ψ_i utilized in the present study are given in Appendix B. There the effect of circumferentially non-uniform tip clearance is incorporated through these characteristics.

A.2 Linearized Equations Governing Stability

The dynamical equations for the compression system are linearized by assuming that each variable can be represented as the sum of a mean and a perturbation,

$$f = \bar{f} + \delta f \quad (\text{A8})$$

After substitution into the governing equations, 2nd-order and higher terms are neglected.

Upstream Duct:

The compressor can create localized flow disturbances, which upstream of the compressor, are of potential form. As experimentally observed these potential disturbances will decay exponentially upstream of the machine. Begin by defining the upstream disturbance velocity potential for the nth-spatial harmonic as

$$\delta\Phi = f(x)e^{i(n\theta + \omega x)} \quad (\text{A9})$$

Based on the assumptions, this must satisfy

$$\nabla^2 \delta\Phi = 0 \quad (\text{A10})$$

for the upstream decaying perturbations. Hence

$$\delta\Phi(x, \theta, t) = a_n e^{n|x/r| + i(n\theta + \omega x)} \quad (\text{A11})$$

This is related to the upstream flow coefficient perturbation by

$$\delta\phi = \frac{\partial}{\partial x}(\delta\Phi) = \frac{|n|}{r} \delta\Phi \quad (\text{A12})$$

The governing equation for the flow in the upstream duct is the linearized unsteady momentum equation,

$$\frac{1}{U} \frac{\partial}{\partial t}(\delta\Phi) + \frac{\delta P_t}{\rho U^2} = \text{Constant} \quad (\text{A13})$$

or substituting (A12), at the compressor inlet,

$$\left. \frac{\delta P_t}{\rho U^2} \right|_2 = -\frac{1}{|n|} \frac{r}{U} \frac{\partial}{\partial t}(\delta\Phi_2) \quad (\text{A14})$$

In addition to (A14), the boundary condition of time independent total pressure at the upstream inlet must also be invoked.

Compressor:

Following the work of Moore and Greitzer [15] and Hynes and Greitzer [18], a model based on one-dimensional flow through the compressor can be developed. The unsteady pressure rise based on this is given by,

$$\frac{P_3 - P_{t1}}{\rho U^2} = \psi_i - L_r - L_s - \lambda \frac{\partial \phi}{\partial \theta} - \frac{\mu r}{U} \frac{\partial \phi}{\partial t} \quad (\text{A15})$$

$$\mu = \left[\sum_{i=1}^N (T_{r,i} + T_{s,i}) + T_{IGV,i} \right] \frac{U}{r} \quad (\text{A16})$$

Linearizing this relation yields,

$$\frac{\delta P_3 - \delta P_{t1}}{\rho U^2} = \frac{d\bar{\psi}_i}{d\phi} \delta \phi - \delta L_r - \delta L_s - \lambda \frac{\partial(\delta \phi)}{\partial \theta} - \frac{\mu r}{U} \frac{\partial(\delta \phi)}{\partial t} \quad (\text{A17})$$

where

$$\bar{\psi}_i = \bar{\psi} + \bar{L}_r + \bar{L}_s \quad (\text{A18})$$

As stated in Chapter 2, the blade row unsteady viscous response models employed in the present investigation are simple first order lags which account for the finite time required for the development of loss within the compressor. For the stator, the transient stagnation pressure loss perturbation is given by,

$$\tau_s \frac{\partial(\delta L_s)}{\partial t} = \frac{\partial \bar{L}_s}{\partial \phi} \delta \phi - \delta L_s \quad (\text{A19})$$

Similarly, the rotor transient stagnation pressure loss is,

$$\tau_r \left(\frac{\partial(\delta L_r)}{\partial t} + \frac{U}{r} \frac{\partial(\delta L_r)}{\partial \theta} \right) = \frac{\partial \bar{L}_r}{\partial \phi} \delta \phi - \delta L_r \quad (\text{A20})$$

Note that the loss generation time constants, τ_s and τ_r , are on the order of the blade row flow through time. Equations (A17) - (A20) are the linearized equations governing the compressor dynamic response.

Downstream Duct:

In the exit duct, there are both convected vortical disturbances and downstream decaying potential perturbations. For axial exit flow from the compressor through a high solidity exit blade row, the axial momentum equation is,

$$\frac{1}{U} \frac{\partial}{\partial t} (\delta\phi) = -\frac{\partial}{\partial x} \left(\frac{\delta P}{\rho U^2} \right) \quad (\text{A21})$$

The exit pressure field perturbations must decay axially downstream (i.e. $\nabla^2 \delta P = 0$), hence they will have a form similar to (A11). Based on this,

$$\frac{\partial}{\partial x} \left(\frac{\delta P}{\rho U^2} \right) = -\frac{|n|}{r} \frac{\delta P}{\rho U^2} \quad (\text{A22})$$

or, at the compressor discharge,

$$\left. \frac{\delta P}{\rho U^2} \right|_3 = \frac{1}{|n|} \frac{r}{U} \frac{\partial}{\partial t} (\delta\phi_3) \quad (\text{A23})$$

Equation (A23) determines perturbation behavior in the exit flow field.

Plenum and Exit Throttle:

For steady flow the static pressure in the plenum is determined by the throttle setting as given in equation (A7). The flow through the throttle is regarded as being quasi-steady, and disturbances in the throttle are not considered. In addition, it will be assumed that the flow in the plenum is spatially uniform with pressure and density changes being related by an isentropic relationship (see Greitzer [4]). Under these constraints, the linearized continuity equation for the plenum is,

$$\left(4B^2 \cdot \frac{L_{total}}{r} \cdot \frac{i\omega r}{U} + \frac{1}{\phi_3 k_t} \right) \frac{\delta P_4}{\rho U^2} = \delta\phi_3 \quad (\text{A24})$$

The quantity L_{total} is the “effective” compressor length defined as,

$$L_{total} = L_1 + L_2 + \mu r \quad (\text{A25})$$

and B is as defined in equation (2.2).

The compression system model described in Sections (A.1)-(A.2) was coded using Matlab. The original programs were written by Van Schalkwyk [37] to study inlet distortion effects on stability. These codes were extensively rewritten by the author to incorporate both blade row unsteady viscous response and asymmetric tip clearance modeling.

A.3 Linearized Steady Flow with Clearance Asymmetry

As a simple first approximation of the effect of tip clearance asymmetry on the background flow, a linearized analysis was conducted. This analysis provides an indication of the distortion of the steady flow created by the presence of non-uniform clearance.^{A1}

For steady flow through the compressor, equation (A2) gives,

$$\frac{P_3 - P_{t2}}{\rho U^2} = \psi - \lambda \frac{\partial \phi}{\partial \theta} \quad (\text{A26})$$

where $\psi = \psi_i - L_r - L_s$ is the actual pressure rise characteristic of the machine. When asymmetric clearance is present in the compressor, this characteristic will be assumed to be a function of $\phi(\theta)$ and $\varepsilon(\theta)$ where

$$\varepsilon(\theta) = \frac{\text{clearance}}{\text{chord}} \quad (\text{A27})$$

Therefore,

$$\psi = \psi(\phi, \varepsilon) \quad (\text{A28})$$

Combining this with (A26), and linearizing,

$$0 = \frac{\partial \psi}{\partial \phi} \delta \phi + \frac{\partial \psi}{\partial \varepsilon} \delta \varepsilon - \lambda \frac{\partial(\delta \phi)}{\partial \theta} \quad (\text{A29})$$

^{A1} Note that this analysis reflects the situation where clearance affects peak pressure rise capability only.

where the unsteady inlet and exit pressure perturbations are taken to be zero. It will be assumed that the clearance variation and corresponding flow coefficient variation are sinusoids of the form,

$$\begin{aligned}\delta\phi &= A_n e^{in\theta} \\ \delta\varepsilon &= B_m e^{im\theta}\end{aligned}\tag{A30}$$

and substituting these into (A29),

$$\delta\phi = \frac{B_m \left(\frac{\partial\psi}{\partial\varepsilon} \right)}{in\lambda - \left(\frac{\partial\psi}{\partial\phi} \right)} \cdot e^{im\theta}\tag{A31}$$

Thus the non-uniformity of the steady flow within the compressor depends on:

- (i) harmonics of $\delta\phi$ and $\delta\varepsilon$,
- (ii) inertia of fluid in compressor, λ
- (iii) sensitivity of the compressor to clearance, $\frac{\partial\psi}{\partial\varepsilon}$
- (iv) compressor characteristic slope, $\frac{\partial\psi}{\partial\phi}$

Similarly, the corresponding pressure perturbation within the machine is simply,

$$\frac{\delta P}{\rho U^2} = -\phi \delta\phi\tag{A32}$$

The real portions of equations (A31) and (A32) are,

$$\Re(\delta\phi) = \frac{B_m \left(\frac{\partial\psi}{\partial\varepsilon} \right)}{\left[n^2 \lambda^2 + \left(\frac{\partial\psi}{\partial\phi} \right)^2 \right]} \cdot \left[n\lambda \sin(m\theta) + \frac{\partial\psi}{\partial\phi} \cos(m\theta) \right]\tag{A33}$$

$$\Re\left(\frac{\delta P}{\rho U^2} \right) = -\phi \cdot \Re(\delta\phi)\tag{A34}$$

As an example of how the linearized steady flow would distort with clearance asymmetry, consider the following case. For a multi-stage compressor having a single

harmonic (180°) casing asymmetry, operating at the peak of the characteristic, with the clearance sensitivity found by Smith [6], assume,

$$\phi = 0.5, \lambda = 1, m = 1, \frac{\partial \psi}{\partial \varepsilon} = -5, \frac{\partial \psi}{\partial \phi} = 0 \quad (\text{A35})$$

Define a clearance asymmetry equal to 2% of chord,

$$B_m = \|\delta \varepsilon\| = 0.02 \quad (\text{A36})$$

From (A33)-(A36), for the first spatial harmonic of the flow distortion,

$$\begin{aligned} \Re(\delta \varepsilon) &= (0.02) \cos \theta \\ \Re(\delta \phi) &= (-0.10) \sin \theta \\ \Re\left(\frac{\delta P}{\rho U^2}\right) &= (0.05) \sin \theta \end{aligned} \quad (\text{A37})$$

These results show that at the peak of the characteristic, the flow coefficient non-uniformity is out of phase with the clearance variation. Therefore, as tip clearance becomes smaller, the flow increases, and as the clearance opens, the flow decreases. This trend agrees with the experimental data shown in Chapter 2. Thus, the linearized analysis has obtained the qualitative variations seen in practice.

Appendix B

Formulation of Compressor Characteristics

In this appendix the mathematical development of the actual and isentropic pressure rise characteristic with clearance asymmetry is presented.

Data such as that of Wisler [9] and McDougall [11] show that in general the variation of characteristics with clearance change is as illustrated in Figure (B1). In this schematic regions with smaller than nominal clearance are characterized by higher pressure rise, while regions with larger than nominal clearance produce lower pressure rise. The nominal tip clearance pressure rise characteristic has its peak at $(\bar{\phi}_p, \bar{\psi}_p)$.

B.1 Baseline Characteristics

Assume that the typical pressure rise characteristic can be adequately represented by a generalized cubic polynomial,

$$\psi(\phi) = A\phi^3 + B\phi^2 + C\phi + D \quad (\text{B1})$$

where the constants are to be determined.

To place the characteristic peak at a point (ϕ_p, ψ_p) , the slope of the cubic must be identically zero there, hence

$$\left. \frac{\partial \psi}{\partial \phi} \right|_{\phi_p} = 3A\phi_p^2 + 2B\phi_p + C \equiv 0 \quad (\text{B2})$$

or, solving for A,

$$A = -\frac{(2B\phi_p + C)}{3\phi_p^2} \quad (\text{B3})$$

In addition, at the peak ,the pressure rise is also specified, so substituting (B3) into (B1)

$$\psi_p = \frac{1}{3}B\phi_p^2 + \frac{2}{3}C\phi_p + D \quad (\text{B4})$$

and solving for D ,

$$D = \psi_p - \frac{1}{3}\phi_p(2C + B\phi_p) \quad (\text{B5})$$

Now A and D are determined in terms of B and C . To further reduce the number of free parameters and form characteristics of a realistic nature, a hinge point must also be specified. For the nominal characteristic this is the point $(\bar{\phi}_m, \bar{\psi}_m)$ in Figure (B1). Specification of the hinge allows B or C to be obtained. In the present case it has proven most effective to solve for C in terms of B , hence from (B1), (B3) and (B5) evaluated at some (ϕ_m, ψ_m) ,

$$\psi_m = -\frac{(2B\phi_p + C)}{3}\phi_m^3 + B\phi_m^2 + C\phi_m + \psi_p - \frac{1}{3}\phi_p(2C + B\phi_p) \quad (\text{B6})$$

or solving for C ,

$$C = \frac{3\phi_p^2(\psi_p - \psi_m) - 2B\phi_p\phi_m^3 + 3B\phi_p^2\phi_m^2 - B\phi_p^4}{\phi_m^3 - 3\phi_p^2\phi_m + 2\phi_p^3} \quad (\text{B7})$$

Therefore, the cubic characteristic passing through a peak at (ϕ_p, ψ_p) and a hinge point at (ϕ_m, ψ_m) is given by equation (B1) with coefficients A , C , and D specified by (B3), (B5) and (B7) respectively. The constant B was chosen through iteration to obtain the desired (i.e. representative) characteristic shape.

Once the characteristic is determined it is often useful to compute the radius of curvature at its the peak. Using the definition of radius of curvature with $\partial\psi/\partial\phi = 0$ it can be shown that the peak radius is,

$$r_p = \frac{1}{|\partial^2\psi/\partial\phi^2|} = \frac{1}{|6A\phi_p + 2B|} \quad (\text{B8})$$

B.2 Characteristics with Tip Clearance Asymmetry

Compressor data illustrates that clearance changes affect both the pressure rise and the flow coefficient associated with the peak of the characteristic. The following equations

were developed to modulate the peak pressure rise in a manner which depends upon the clearance geometry, the size of the asymmetry, and the sensitivity of the compressor to clearance changes. Note that $\bar{\psi}_p$ is specifically the peak pressure rise of the nominal clearance characteristic hence,

$$\psi_p = \bar{\psi}_p \cdot \left\{ 1 + \left| \frac{\partial \psi}{\partial \varepsilon} \right| \delta \varepsilon \cdot f(\theta) \right\} \quad (\text{B9})$$

where $\delta \varepsilon$ = maximum amplitude of the asymmetry

$f(\theta)$ = shape of clearance geometry (e.g. $\cos(\theta)$)

$\left| \frac{\partial \psi}{\partial \varepsilon} \right|$ = sensitivity of compressor pressure rise to clearance change (from data)

In addition, the asymmetric clearance characteristic peaks must also be shifted such that the higher peaks occur at lower flow coefficients. This was accomplished through shifts of the nominal characteristic peak flow coefficient,

$$\phi_p = \bar{\phi}_p \cdot \{1 - k \cdot f(\theta)\} \quad (\text{B10})$$

where k is determined from data, or by aligning the peaks on a line of specified angle β as shown in Figure (B1). In the latter case the value of k is obtained from,

$$k = \frac{\bar{\psi}_p \delta \varepsilon}{\bar{\phi}_p \tan(\beta)} \cdot \left| \frac{\partial \psi}{\partial \varepsilon} \right| \quad (\text{B11})$$

Similarly, in Figure (B1), the hinge point flow coefficient is also shifted by a small amount, hence

$$\phi_m = \bar{\phi}_m \cdot \{1 + m \cdot f(\theta)\} \quad (\text{B12})$$

where m is typically determined by iteration. Note that the shift in the hinge point is in the opposite direction of the peak shift. Also, the hinge point pressure rise is not modulated hence $\psi_m = \bar{\psi}_m$.

By combining relations (B9), (B10) and (B12) with the cubic characteristic defined previously, various families of characteristics can be readily generated. Two examples are shown in Figures (2.4) and (2.5).

B.3 Isentropic Characteristics

The isentropic characteristics utilized in this study were not developed from the blading geometry of any particular compressor, but were formulated to include shifts due to different levels of clearance. For simplicity it will be assumed that the isentropic total-to-static characteristic is approximately linear,

$$\psi_i = E\phi + G \quad (\text{B13})$$

Based on stall margin constraints, the nominal compressor design point is specified at $(\bar{\phi}_d, \bar{\psi}_d)$ with efficiency η . The definition of efficiency utilized here is,

$$\eta = \frac{\bar{\psi}_d}{\psi_i} \quad (\text{B14})$$

so by combining (B13) and (B14),

$$G = \frac{1}{\eta} \bar{\psi}_d - E\bar{\phi}_d \quad (\text{B15})$$

In addition, it will be assumed that at the design point the slope of the isentropic characteristic is approximately equal to that of the actual characteristic. Therefore,

$$E = \left. \frac{\partial \psi}{\partial \phi} \right|_{\bar{\phi}_d} = 3A\bar{\phi}_d^2 + 2B\bar{\phi}_d + C \quad (\text{B16})$$

where A , B and C were previously specified for each characteristic in the family.

To determine the efficiency of the compressor at a particular level of clearance, the formulation proposed by Smith [35] was utilized. Smith's result accounts for both the blockage and tangential force defect in the endwall region, and was originally developed to compute compressor efficiency based on cascade measurements. Smith [35] defines,

$$\eta = \tilde{\eta} \cdot \frac{\left(1 - \frac{\delta_h^* + \delta_t^*}{h}\right)}{\left(1 - \frac{v_h + v_t}{h}\right)} \quad (\text{B17})$$

where cascade efficiency is denoted by $\tilde{\eta}$, while δ^* and v represent the actual endwall

flow displacement thickness and tangential force defect respectively. In the worst case, the endwall flow will provide no tangential force on the blading ($F_u = 0$), hence from [35],

$$v_h = \frac{1}{r_h \bar{F}_{uh}} \int_{r_h}^{r_h + \delta_h} (\bar{F}_u - F_u) r dr = \frac{1}{r_h} \int_{r_h}^{r_h + \delta_h} r dr \quad (\text{B18})$$

so,

$$v_h \approx \delta_h$$

and similarly at the tip,

$$v_t \approx \delta_t$$

As a first approximation based on data, assume,

$$\begin{aligned} v_{h,t} &\approx \delta_{h,t} \approx 1 \text{ clearance height} \\ \delta_{h,t}^* &\approx 3\delta_{h,t} \approx 3 \text{ clearance heights} \end{aligned} \quad (\text{B19})$$

Therefore, using (B19), (B17) the efficiency is,

$$\eta \approx \bar{\eta} \cdot \frac{\left(1 - \frac{6\varepsilon}{AR}\right)}{\left(1 - \frac{2\varepsilon}{AR}\right)} \quad (\text{B20})$$

where the clearance has been normalized by chord, and AR is the blade aspect ratio. Note that with clearance asymmetry the efficiency will vary around the annulus since ε is a function of θ .

In summary, the isentropic characteristics with clearance asymmetry are obtained by combining (B13) and (B15),

$$\psi_i = (\phi - \bar{\phi}_d) \frac{\partial \psi}{\partial \phi} \Big|_{\bar{\phi}_d} + \frac{1}{\eta} \bar{\psi}_d \quad (\text{B21})$$

where the derivative is given by (B16) and efficiency is approximated from (B20).

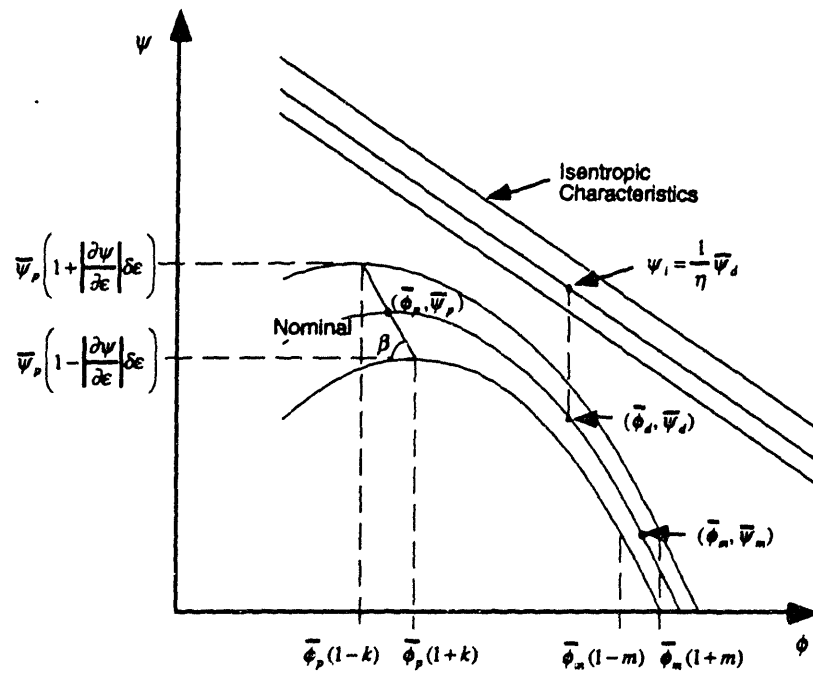


Figure (B.1): Schematic of actual and isentropic compressor pressure rise characteristics

THESIS PROCESSING SLIP

FIXED FIELD: ill _____ name _____

index _____ biblio _____

► COPIES: Archives Aero Dewey Eng Hum
Lindgren Music Rotch Science

TITLE VARIES: ► _____

NAME VARIES: ► _____

IMPRINT: (COPYRIGHT) _____

► COLLATION: 682

► ADD. DEGREE: _____ ► DEPT.: _____

SUPERVISORS: _____

NOTES:

cat'r: _____ date: _____

► DEPT: Aero page: J12L

► YEAR: 1976 ► DEGREE: M.S.

► NAME: GRAF, Martin Bowyer